

## ABSTRACT

Title of Document:                   TEMPORAL ANALYSIS OF HYDROXYL  
RADICAL SCAVENGING IN WATERS.

Joel Edward Donham, Master of Science, 2013

Directed By:                         Assistant Professor Dr. Krista Rule Wigginton,  
Civil and Environmental Engineering

The ability to assess hydroxyl radical ( $\bullet\text{OH}$ ) scavenging rates of natural organic matter (NOM) ( $k_{\text{NOM},\bullet\text{OH}}$ ) is necessary for the optimization of advanced oxidation processes (AOPs) for water treatment, and to understand the role of  $\bullet\text{OH}$  in natural systems. We have developed a rapid method to measure  $\bullet\text{OH}$  scavenging rates in less than one hour. Using the method, we measured  $k_{\text{NOM},\bullet\text{OH}}$  for NOM isolates, and performed the first known scavenging analyses of surface waters and treated drinking waters over time. The results are compared with values quantified using more time consuming methods. Our results reveal that  $k_{\text{NOM},\bullet\text{OH}}$  in water samples can fluctuate with time, which has implications for AOP operation. The methods and benefits of the new measurement technique and implications of observed variability of  $k_{\text{NOM},\bullet\text{OH}}$  values on AOP operations are presented. Additionally, observations regarding current NOM scavenging measurement and analysis methods are discussed.

TEMPORAL ANALYSIS OF HYDROXYL RADICAL SCAVENGING IN  
WATERS.

By

Joel Edward Donham

Thesis submitted to the Faculty of the Graduate School of the  
University of Maryland, College Park, in partial fulfillment  
of the requirements for the degree of  
Master of Science  
2013

Advisory Committee:  
Professor Dr. Krista Rule Wigginton, Chair  
Dr. Erik Rosenfeldt  
Professor Dr. Baoxia Mi

© Copyright by  
Joel Edward Donham  
2013

## Preface

To Grace, thanks for all the support!

## Acknowledgements

Thanks to Krista Wigginton, Erik Rosenfeldt, Baoxia Mi, Paul Richardson, Steve Davidson, Neil Blough and Robert Mutel, for hearing me out.

# Table of Contents

<b>Dedication .....</b>	<b>ii</b>
<b>Acknowledgements .....</b>	<b>iii</b>
<b>Table of Contents .....</b>	<b>iv</b>
<b>List of Tables .....</b>	<b>vi</b>
<b>List of Figures.....</b>	<b>vii</b>
<b>Chapter 1: Introduction .....</b>	<b>1</b>
<b>Chapter 2: Analysis of Hydroxyl Radical Scavenging Variability in Water Treatment .....</b>	<b>7</b>
<b>2.1 Abstract .....</b>	<b>7</b>
<b>2.2 Introduction.....</b>	<b>8</b>
<b>2.3 Materials and Methods.....</b>	<b>12</b>
2.3.1 Investigated waters .....	12
2.3.2 Chemicals .....	13
2.3.3 RBS equipment .....	14
2.3.4 Analytical methods.....	15
<b>2.4 Results and Discussion .....</b>	<b>15</b>
2.4.1 Scavenging rate measurements .....	15
2.4.2 Scavenging variability in water treatment systems .....	18
2.4.3 Impacts of scavenging variability on energy consumption and assurance of treatment in advanced oxidation processes .....	23
<b>2.5 Conclusions.....</b>	<b>26</b>
2.5.1 Scavenging variability dependent on sampling location.....	26
2.5.2 The R-SAM method has applications in real-time control of AOP systems.....	27
<b>2.6 Chapter 2 Supporting Information.....</b>	<b>28</b>
<b>2.7 Chapter 2 References .....</b>	<b>28</b>
<b>Chapter 3: Photometric Hydroxyl Radical Scavenging Analysis of Standard NOM Isolates.....</b>	<b>32</b>
<b>3.1 Abstract .....</b>	<b>32</b>
<b>3.2 Introduction.....</b>	<b>32</b>
<b>3.3 Materials and Methods.....</b>	<b>35</b>
3.3.1 Chemicals .....	35

3.3.2	Investigated isolates .....	35
3.3.3	R-SAM equipment .....	36
<b>3.4</b>	<b>Results .....</b>	<b>37</b>
3.4.1	Selection of probe compound and optimization of NOM scavenging measurement method.....	37
3.4.2	Rate constants for reaction of •OH with NOM isolates .....	41
<b>3.5</b>	<b>Discussion .....</b>	<b>43</b>
3.5.1	Comparison with previous results .....	43
3.5.2	Correlation of $k_{\bullet\text{OH}, \text{NOM}}$ with NOM characteristics .....	44
3.5.3	Implications of transport limits on fast reactions for competition kinetics based scavenging analysis .....	47
<b>3.6</b>	<b>Conclusions.....</b>	<b>48</b>
<b>3.7</b>	<b>Chapter 3 Supporting Information.....</b>	<b>50</b>
<b>3.8</b>	<b>Chapter 3 References .....</b>	<b>52</b>
<b>Chapter 4: Conclusions .....</b>		<b>54</b>
<b>Comprehensive Bibliography .....</b>		<b>62</b>
<b>Appendix: Detailed R-SAM procedure.....</b>		<b>56</b>

## List of Tables

Table 1: Methylene blue and sodium fluorescein probe dye structures (Sigma Aldrich Co. LLC, 2013) and other parameters. ....	40
Table 2: NOM isolates studied. ....	42
Table 3: Reaction rates constants of compounds used in competition kinetics based scavenging analyses. ....	48
Table 4: R-SAM measurement t-BuOH mixing volumes.....	59



## List of Figures

<p>Figure 1: The impact of measured NOM, carbonate species, and modeled trace contaminant (EE2) concentration on a the contaminant’s proportional •OH consumption. Reaction rates with NOM, carbonate species and EE2 obtained from the present work, (Hoigne et al., 1985) and (Rosenfeldt et al., 2004) respectively. ....</p>	4
<p>Figure 2: Plant 1 sampling locations at influent and post-filtration, and Plant 2 sampling location after settling, prior to filtration. ....</p>	13
<p>Figure 3: Schematic of R-SAM setup consisting of an AvaSpec-2048 fiber optic spectrophotometer, AvaLight-HAL tungsten halogen light source and AvaSoft software (Avantes Inc.), custom wooden lamp housing, standard florescent garage work light (HDX) with two 13 W low-pressure ultraviolet bulbs (Phillips Inc. # TUV PL-S 13W/2P), custom beaker holder with fiber optic ports for the spectrometer, standard laboratory stir plate, 100 mL beaker, 10 mm stir-bar (Fisher Scientific Inc), and vinyl shutter plate to start and stop UV exposure. UV fluence was measured at 30 (+/- 5) <math>\mu\text{W}/\text{cm}^2</math> using methods presented in (Bolton et al., 2003). Spectrometer data were compiled with Microsoft <i>Excel</i> and processed with GraphPad <i>Prism</i>. ....</p>	14
<p>Figure 4: Measured scavenging at lab-filtered Site 1 infulent and post-filtration water. Measured scavenging apportioned between NOM and carbonate scavenging, based on alkalinity, pH and published carbonate and bicarbonate •OH reaction rate constants. TOC is also shown. ....</p>	19
<p>Figure 5: Site 1 measured <math>k_{\text{OH,NOM}}</math> values determined by subtracting calculated carbonate scavenging and normalizing with TOC. <math>k_{\text{OH,NOM}}(\text{filtered})= 2.0 \pm 1.0 \times 10^8</math> <math>k_{\text{OH,NOM}}(\text{raw, excluding first two samples})= 2.0 \pm 0.7 \times 10^8</math>. ....</p>	20
<p>Figure 6: Measured background scavenging in Plant 2 water post coagulation-flocculation and settling, prior to final filtration. Scavenging was evaluated in lab filtered sample water and water as sampled to gauge the effects of filterable constituents. ....</p>	22
<p>Figure 7: Plant 2 NOM concentration in lab filtered and as sampled water. ....</p>	22
<p>Figure 8: Measured Plant 2 <math>k_{\text{OH,NOM}}</math> values indicate significant variability over a factor of 3 indicating a highly variable water matrix. ....</p>	23

Figure 9: NOM scavenging in Plant 2, and two operational strategies for addressing scavenging in AOP treatment: constant scavenging assumption (green), and a proposed real-time feedback strategy based on the R-SAM protocol (red).....	26
Figure 10: Municipal scale UV/H <sub>2</sub> O <sub>2</sub> operations and maintenance annual costs.....	28
Figure 11: NOM adsorption and UV decay in methylene blue and fluorescein.....	39
Figure 12: Measured rate constants for NOM isolates by researcher and measurement method; Fl. R-SAM: fluorescein based R-SAM, MB R-SAM: methylene blue R-SAM, SCN-: thiocyanate competition kinetics, DG 400/272: direct measurement of transient DOM radicals at 272 and 400 nm.....	42
Figure 13: Consistant second order degradation of MB to 80% decay. Minimal photodecay (at 0 mg/L H <sub>2</sub> O <sub>2</sub> ) indicates resistance to UV <sub>254</sub> . Linear decay curves at higher H <sub>2</sub> O <sub>2</sub> concentrations indicates predicatable second order behavior when reacting with •OH, and limited generation of •OH scavenging byproducts. ....	50
Figure 14: Consistant second order degradation of fluorescein (Fl.) to 30% decay. Indicates predicatable second order behavior when reacting with •OH, and limited generation of •OH scavenging byproducts. ....	50
Figure 15: Correlation of NOM characteristics with •OH scavenging rate constants. : PLFA-R NOM. In most cases any apparant relationship between the NOM characteristic shown and the Molar-carbon •OH scavenging rate was only due to inclusion of the PLFA-R outlier. ....	51

## Chapter 1: Introduction

Hydroxyl radical ( $\bullet\text{OH}$ ) oxidation plays a crucial role in natural systems as a terminal oxidizer involved in chemical fate and transport, and elemental cycling (Hynes et al. 1986; Sinkkonen et al., 2000). In biotic systems, radical chemistry, including  $\bullet\text{OH}$ , is blamed for health effects ranging from cancer to tissue aging (Poeggeler et al., 1993; Malins et al., 1993). More recently, oxidation with  $\bullet\text{OH}$  is often extolled as a panacea for water quality concerns ranging from pharmaceutical and personal care products (PPCP) residues in surface water to industrial discharges using a class of treatments termed advanced oxidation processes (AOPs) that use  $\bullet\text{OH}$  as a treatment oxidant (Espulgas et al., 2007; Peternel et al., 2007). While  $\bullet\text{OH}$  is an exceptionally powerful oxidant with a myriad of applications, the roles and applications attributed to this chemical may have outstepped research to understand the major controller of  $\bullet\text{OH}$  concentrations in many natural and engineered systems:  $\bullet\text{OH}$  scavenging by background water constituents. This work will investigate the role of background natural organic matter (NOM) as a  $\bullet\text{OH}$  scavenger; however, the methods developed for this work may be applicable to other  $\bullet\text{OH}$  reactions.

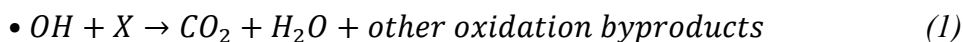
NOM is a blanket term given to soluble organic matter present in natural waters –generally polar or ionic products of the decomposition of organic material. NOM is a highly complex scavenger that has been the subject of extensive research, yet understanding of its reaction characteristics with  $\bullet\text{OH}$  remains elusive (Westerhoff et al., 2007; McKay et al., 2013). In an effort to further the understanding of the scavenging behavior of NOM, the research presented in this thesis (1) developed and refined a rapid photometric scavenging measurement system

(‘R-SAM’) to quickly evaluate scavenging in a variety of systems, (2) conducted long-term sampling studies of scavenging in drinking water before and after treatment to better understand NOM scavenging and its implications for AOPs, and (3) measured scavenging rates in NOM isolate standards to compare with measurements made using other methods and better understand how scavenging varies between different isolates.

The extraordinarily high oxidizing power of •OH makes it an interesting compound from a scientific perspective and attractive from an engineering perspective. For reference, the oxidation potential of •OH is 2.70 eV compared to 1.49 eV for chlorine, the most common oxidant used in water treatment (Dorfman et al., 1973). It therefore has nearly double the power of chlorine to abstract a hydrogen atom from a compound or bond to an unsaturated atom in a compound—two common oxidative degradation mechanisms (Buxton et al., 1988). •OH is often considered ‘non-selective’ due to its ability to react with nearly any compound present in water, including water molecules themselves—although at a very low rate (Stumm et al., 2006). The implication of this reactivity is that, while •OH participates in interesting chemistries relevant to chemical pathways in the environment and contaminant degradation, based on a kinetic analysis, nearly all •OH in many aquatic systems will be consumed in bystander reactions with NOM.

The reactions between •OH and organic compounds result in the generation of carbon dioxide (CO<sub>2</sub>) and water (H<sub>2</sub>O), oxidation byproducts involving organic matter constituents other than carbon, hydrogen and oxygen, and incomplete oxidation of organic structures if insufficient •OH is supplied to completely oxidize the compound

(Equation 1). These reactions are typically modeled using second order kinetics, wherein the rate of the reaction of two species is proportional to the product of the concentrations of each species (compound 'X' and •OH) and a reaction rate constant 'k' (Equation 2).



$$[\bullet OH][X]k_{\bullet OH, X} = \text{rate of consumption of } \bullet OH \text{ or } X \quad (2)$$

Using this relationship, one can consider a hypothetical case in which •OH is employed to remove a trace contaminant (e.g. 50 ng/L ethinyl estradiol (EE2)) during drinking water treatment. EE2 is a birth control hormone often found in wastewater effluent influenced surface waters at ng/L levels (Koplin et al., 1982). The treatment system's conventional coagulation-flocculation, filtration, and chlorination treatments can attain final NOM concentrations of around 2.4 mg/L of carbon (mgC/L) but may be insufficiently effective against EE2 due to its resistance to oxidation, and low effective dose (Westerhoff et al., 2005).

To remove EE2, a hypothetical AOP is employed to generate •OH. However, some •OH is scavenged in reactions with NOM, carbonate species and other benign background constituents. A calculation with measured concentrations of background constituents and published k values demonstrates that background scavengers consume almost all •OH produced (Figure 1). Therefore, scavenging has a large impact on the amount of •OH that must be supplied to the system to treat trace contaminants and must be addressed in AOP system design and operation.

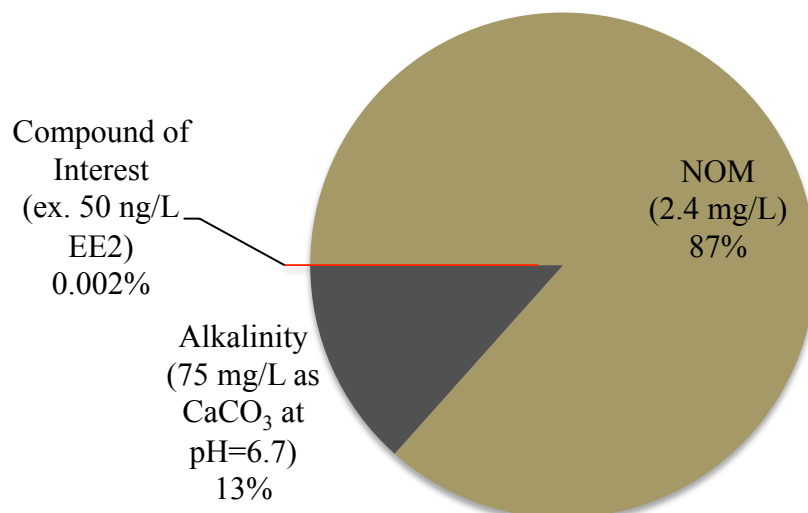


**Figure 1: The impact of measured NOM, carbonate species, and modeled trace contaminant (EE2) concentration on a the contaminant's proportional •OH consumption. Reaction rates with NOM, carbonate species and EE2 obtained from the present work, (Hoigne et al., 1985) and (Rosenfeldt et al., 2004) respectively.**

The consumption of •OH by scavengers is more relevant to the chemistry of a given system in its effect on the hydroxyl radical concentration ([•OH]) available to degrade contaminants, rather than its competitive consumption of •OH. [•OH], however, is nearly impossible to measure directly due to its instability (Buxton et al., 1988). Because •OH is so reactive, its concentration is often defined indirectly as the steady state [•OH] ([•OH]<sub>ss</sub>) by the equilibrium between the •OH production rate ( $\alpha_{\bullet OH}$ ) and the consumption of •OH from scavengers ( $X_i$ ) and compound of interest (A) in solution (Katsoyiannis et al., 2011). [•OH]<sub>ss</sub> is thereby expressed by the steady state hydroxyl radical equation (3).

$$[\bullet OH]_{SS} = \frac{([A]k_{\bullet OH,A} + \sum_i [X_i]k_{\bullet OH,X_i})}{\alpha_{\bullet OH}} \quad (3)$$

where  $k_{\bullet OH,X_i}$  and  $k_{\bullet OH,A}$  are rate constants for the reaction •OH with scavenger  $X_i$  and compound of interest A respectively. In a situation where

scavenging is dominated by NOM (as in most AOP drinking water applications)

Equation (3) approaches:

$$\frac{\alpha_{\bullet OH}}{[NOM]k_{\bullet OH,NOM}} = [\bullet OH]_{SS} \quad (4)$$

Equation (4) demonstrates the inverse relationship between NOM scavenging and  $[\bullet OH]_{SS}$ , for a given  $\alpha_{\bullet OH}$ . Unfortunately, and much to the detriment of research and AOP operation, NOM scavenging rates are highly variable, relatively unpredictable (Westerhoff et al., 2007), and stability of scavenging rates in NOM from a specific origin over time hasn't been evaluated. Research has demonstrated that NOM scavenging rates vary over a factor of 2.4 (Brizonik et al., 1998) or more (McKay et al., 2011; McKay et al., 2013). This level of uncertainty leads to potentially large errors in predicted NOM scavenging requiring substantial estimates in research and large design margins in engineering, when being modeled or predicted. Additionally, due to the laborious and equipment-intensive procedures conventionally used to measure scavenging (Buxton et al., 1995; Katsoyiannis et al., 2011), predictive models are often used to estimate scavenging behavior. Current predictive models for bulk NOM scavenging, however, are only valid within a factor of three. Reliance on these low-precision estimates limits understanding of  $\bullet OH$  systems and affects treatment assurance and efficiency in energy intensive AOP systems.

The present research introduces a high-throughput rapid scavenging analysis method (R-SAM) that is used to determine the operational implications of using predictive scavenging models in AOPs for drinking water, and evaluate alternative methods to addressing scavenging in AOPs. In Chapter 2, this tool is used to evaluate

temporal scavenging variability in water treatment systems as it relates to AOP treatment prospects. In Chapter 3, the tool is used to evaluate the scavenging properties of standard NOM isolates to provide a direct comparison with other scavenging analysis methods, explore the differences in scavenging between various NOM compositions, and gain insight into NOM scavenging measurement methods.



## Chapter 2: Analysis of Hydroxyl Radical Scavenging Variability in Water Treatment

### **2.1 Abstract**

Hydroxyl radical ( $\bullet\text{OH}$ ) scavenging, and specifically natural organic matter (NOM) scavenging has considerable impacts on the efficacy and efficiency of advanced oxidation processes (AOPs) for water treatment. In many natural water systems, NOM scavenging governs the availability of  $\bullet\text{OH}$  to react with pollutants of interest. Significant work has been performed to measure NOM scavenging properties as a function of NOM origin and characteristics, and how differences in scavenging levels affect AOP operation in different source waters. There is little understanding, however, of how NOM scavenging changes over time in a given source, how changes in scavenging could affect AOP operation, and how impacts can be addressed strategically. The present research discusses a novel rapid scavenging analysis method (R-SAM) that is used to evaluate short and long term NOM scavenging behavior as it applies to hypothetical add-on AOP systems in two existing water treatment plants. Results demonstrate that (1) short-term stability of bulk scavenging and NOM scavenging rate constants in partially treated drinking water drawing from a reservoir source, yet considerable variability of bulk scavenging and NOM scavenging rate constants in partially treated water drawing from a more turbulent direct river source with a short term influent holding reservoir; (2) consistent background scavenging reductions and stabilization after coagulation-flocculation, settling and filtration, despite changing influent conditions; (3) seasonal changes in NOM loading that were observed to have a greater impact on bulk scavenging rates compared with observed variability in scavenging rate constants;

and (4) an operational strategy that employs real-time scavenging analysis could reduce energy consumption in AOP Treatment by 41% while increasing treatment reliability.

## ***2.2 Introduction***

Public concern, and in some cases, potential future regulations regarding emerging trace contaminants, unpleasant taste and odor producing compounds, and algal toxins in drinking water are motivating water utilities to incorporate advanced oxidation processes (AOPs) into existing treatment trains (Rosenfeldt et al., 2004; Comninellis et al., 2008). Emerging trace organic contaminants of concern include endocrine disrupting compounds (EDCs) found in pharmaceutical and personal care products (PPCPs), pesticides, and animal husbandry hormones used in agriculture (Kolpin et al., 2002). Traditional water treatment processes, such as coagulation-flocculation, filtration, and chlorination are designed to remove turbidity and inactivate biological agents, but do little to address trace organic contaminants (Westerhoff et al., 2005).

Because standard treatment processes are not sufficiently effective at removing trace contaminants, concentrations of trace contaminants in water systems may increase over time. As urban areas continue to grow throughout the world, water reuse cycles will continue to shorten. Shorter reuse cycles have the potential to cause trace contaminants to build up in drinking water sources increasing the need to address emerging contaminants (Espulgas et al, 2007). AOPs can supplement traditional water treatment with powerful radical oxidants, most commonly the

hydroxyl radical ( $\bullet\text{OH}$ ), that are capable of treating most trace contaminants and preventing contaminant buildup in regional water systems (EPA, 1998).

Despite their potential, there are still some complications to implementing AOPs related to current difficulties in evaluating  $\bullet\text{OH}$  scavenging by natural organic matter (NOM). Specifically, it is complicated to measure  $\bullet\text{OH}$  scavenging levels, predictive scavenging models have limited precision, and there is no evidence as to the stability of scavenging levels over time—limiting the credibility of pilot study measurements. The result of these difficulties is that  $\bullet\text{OH}$  scavenging cannot be accurately determined at the time and point of treatment. Without accurate knowledge of scavenging levels AOPs must be operated at high levels of  $\bullet\text{OH}$  production to address the highest foreseeable scavenging levels or risk insufficient treatment caused by higher than expected scavenging. Operating at unnecessarily high levels of  $\bullet\text{OH}$  production to accommodate uncertainty in NOM scavenging may lead to significant increases in energy use and cost associated with AOPs due to the energy intensive nature of common  $\bullet\text{OH}$  production methods.

$\bullet\text{OH}$  used in AOPs is generated in numerous ways including as a byproduct of ozone ( $\text{O}_3$ ) treatment, the reaction of hydrogen peroxide ( $\text{H}_2\text{O}_2$ ) with  $\text{O}_3$  ( $\text{O}_3/\text{H}_2\text{O}_2$ ), UV photolysis of  $\text{O}_3$  (UV/ $\text{O}_3$ ), UV photolysis of  $\text{H}_2\text{O}_2$  (UV/ $\text{H}_2\text{O}_2$ ), UV photocatalysis using  $\text{TiO}_2$  or  $\text{ZnO}_2$  (UV/ $\text{TiO}_2$  or UV/ $\text{ZnO}_2$ ), photo-Fenton processes, radiolysis, sonolysis and non-thermal plasma processes (U.S. EPA, 1998; Comninellis et al., 2008; Peternel et al., 2007; Buxton et al., 1988; Hao et al., 2006). These processes range in their level of development and potential application. UV/ $\text{H}_2\text{O}_2$  for example is an established technology currently implemented at the municipal scale to address

emerging, but as yet unregulated contaminants (Tucson Water, 2012) as well as algal toxins, and taste and odor concerns (Trojan Technologies Inc., 2005). In contrast, UV/TiO<sub>2</sub> AOPs are an emerging technology being developed and refined for distributed solar powered water disinfection and contaminant degradation (SODIS) in the developing world (Moncayo-Lasso et al., 2012), while radiolysis is used primarily for research purposes (Asmus, 1984).

•OH is successful in degrading trace contaminants because of its high oxidizing power. For comparison, the standard oxidation potential of hydroxyl radicals is 2.70 eV compared to 1.49 eV for chlorine, the most common oxidant used in water treatment (Dorfman et al., 1973). This high electron affinity allows •OH to be considered ‘non-selective’ due to its ability to instantaneously oxidize nearly any organic compound present in water, and even water molecules themselves –although at a very low rate (Stumm et al., 1996).

An implication of this high reactivity is that numerous benign water constituents will scavenge •OH, including NOM and carbonate species (Lee et al., 2010). High scavenging levels can have a significant effect on •OH concentrations available to degrade target pollutants; consequently, higher background scavenging levels must be addressed by increasing the •OH production rate in AOPs, with consequent increases in energy and chemical costs (Katsoyiannis et al., 2011). AOP systems must be designed to accommodate expected scavenging levels to ensure complete treatment without producing excessive amounts of •OH and thus increased costs, air emissions, and resource consumption. Determining expected scavenging levels requires either predictive modeling or direct measurement.

The scavenging behavior of NOM, which can contribute more than 90% of scavenging (present work), is particularly difficult to predict due to its complex and highly variable composition. NOM concentration, as measured by total organic carbon content (TOC), has proven to be a poor predictor of NOM scavenging rates due to the variability of NOM- $\bullet$ OH reaction rate constants (Katsoyiannis et al., 2011; Westerhoff et al., 1999; McKay et al., 2011). Additionally more detailed NOM characteristics such as carbon aromaticity and elemental composition have demonstrated little correlation with scavenging rate constants as well (Westerhoff et al., 2007; McKay et al., 2013). Combining the individual effects of numerous organic matter variables to predict scavenging rates, however, has resulted in some success. A multivariate model of SUVA<sub>254</sub>, dispersity, hydrophobicity, hydrophilicity/anionic character, and the ratio of the fluorescence emission intensity at 450 nm to that at 500 nm after excitation at 370 nm (a correlate of aquatic versus terrestrial origins of the organic matter) has shown potential to predict the scavenging rate of wastewater effluent organic matter (EfOM) with considerable accuracy (Rosario-Ortiz et al., 2008). This method, however, has not been validated for use with NOM and requires extensive organic matter evaluation to predict scavenging behavior.

Some researchers have directly measured scavenging behavior in candidate treatment waters to determine impacts on AOP design. Katsoyiannis and associates (2011), for example, demonstrated variability of over 300% in scavenging rates and 75% in  $k_{\text{OH,NOM}}$  values among different surface waters. Because AOPs must be designed to address an expected level of scavenging; the observed scavenging

variability highlights a need to better understand scavenging variability in candidate waters prior to AOP implementation.

While discrete measurements and multivariate models have demonstrated success in typifying scavenging at a single point in time, there is little understanding of how properties related to NOM scavenging generally behave over time. Research has shown evidence of seasonal changes in NOM composition (Sharp et al., 2006); hence, discrete evaluations of NOM scavenging behavior using scavenging measurements or predictive models may not be accurate over time.

This study aims to evaluate how scavenging levels change over time in the context of drinking water treatment plants where AOP systems may be employed. A rapid scavenging analysis method (R-SAM) was developed and optimized for this purpose. The potential impact of constant scavenging AOP design assumptions on operational costs and treatment consistency was evaluated using R-SAM data.

## ***2.3 Materials and Methods***

### **2.3.1 Investigated waters**

Samples were collected from two mid-Atlantic water treatment plants with river water sources. Both plants employed coagulation, rapid mix, flocculation, settling and filtration. Plant 1 (6.0 million gallons per day [MGD] capacity) draws from a river-fed large capacity reservoir source and Plant 2 (180 MGD) draws directly from a river source with a short-term ( $\approx 2$  week) influent holding reservoir. Based on the configuration of sample taps in each treatment train, water was sampled at two points in Plant 1 (influent and after filtration), and at one point in Plant 2 (after settling but prior to filtration) (Figure 2).

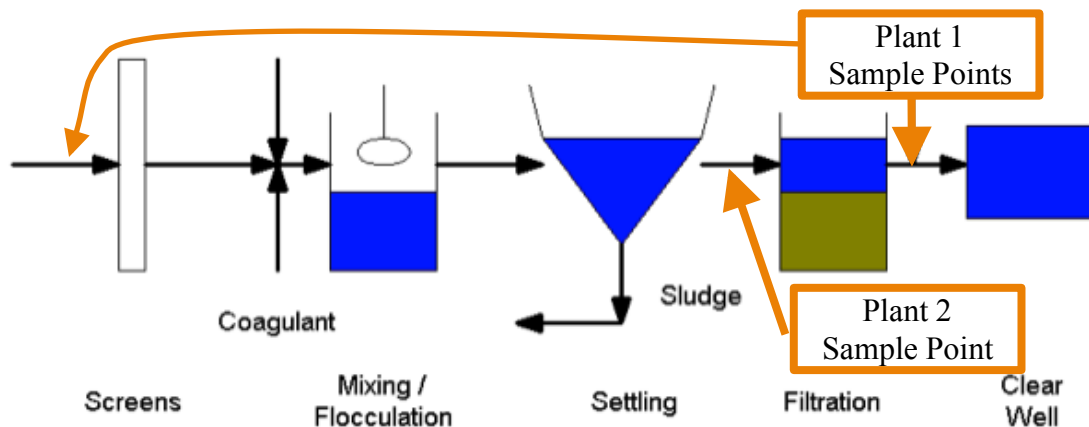


**Figure 2: Plant 1 sampling locations at influent and post-filtration, and Plant 2 sampling location after settling, prior to filtration.**

Samples were collected in 1.0 L amber glass bottles with Teflon-lined lids and minimal headspace. Immediately after collection, samples were stored in a cooler at 4°C and transported to the laboratory. They were then allowed to equilibrate to room temperature before analysis. All Plant 1 water was vacuum filtered using 1.2 μM glass fiber filters prior to R-SAM analysis to reduce the effects of entrained particulate matter. Plant 2 water was analyzed before and after 1.2 μM vacuum filtration to gauge the effects of filterable material. All analysis was performed within 48 hours of sampling, as scavenging rates were observed to decline after more than 48 hours of storage at 4°C.

### 2.3.2 Chemicals

Methylene blue (MB), hydrogen peroxide (H<sub>2</sub>O<sub>2</sub>), isopropyl alcohol (IPA), tertiary butyl alcohol (t-BuOH), and sodium hydroxide (NaOH) were obtained from Thermo Fisher Scientific Inc. (Waltham, Massachusetts) and used as received.

### 2.3.3 RBS equipment

The RBS system consisted of a UV reactor with perpendicular real-time absorbance measurement capabilities (Figure 3). A UV/H<sub>2</sub>O<sub>2</sub> process in the reactor generates •OH causing an added probe dye to degrade and disappear at a rate proportional to background scavenging and the concentration of t-BuOH doped in solution. The probe dye degradation rate at various concentrations of t-BuOH is measured by the spectrophotometer and used to determine the scavenging rate as discussed in section 2.3.1.

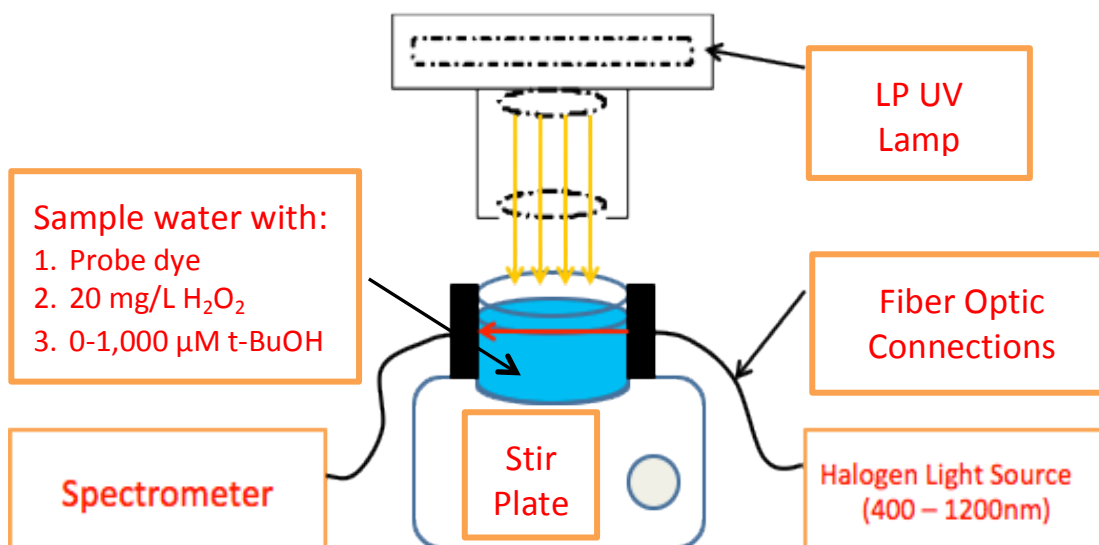


**Figure 3: Schematic of R-SAM setup consisting of an AvaSpec-2048 fiber optic spectrophotometer, AvaLight-HAL tungsten halogen light source and AvaSoft software (Avantes Inc.), custom wooden lamp housing, standard florescent garage work light (HDX) with two 13 W low-pressure ultraviolet bulbs (Phillips Inc. # TUV PL-S 13W/2P), custom beaker holder with fiber optic ports for the spectrometer, standard laboratory stir plate, 100 mL beaker, 10 mm stir-bar (Fisher Scientific Inc), and vinyl shutter plate to start and stop UV exposure. UV fluence was measured at 30 (+/- 5)  $\mu\text{W}/\text{cm}^2$  using methods presented in (Bolton et al., 2003). Spectrometer data were compiled with Microsoft *Excel* and processed with GraphPad *Prism*.**

To evaluate the potential for thermal impacts on R-SAM measurements, heating inside the R-SAM reactor was measured. A temperature increase of <1 °C was observed during UV exposure in solutions of probe dye and NOM at typical test



concentrations and duration. This minute level of heating should cause less than 2% elevation in NOM reaction rate constants based on thermodynamic variables in (McKay et al., 2011). •OH scavenging rates of the probes and variable competitors could also be affected by heating, but due to the minimal heating observed, and subsequent minimal impact on system behavior, these potential effects were ignored.

### **2.3.4 Analytical methods**

pH was measured at the time of sampling with an AP84 pH meter (Thermo Fisher Scientific Inc.). Carbonate speciation was determined using pH, the  $pK_a$  values of the carbonate system (7.9 and 4.8), and alkalinity (Stumm et al., 2006). Alkalinity was measured after returning to the laboratory with standard procedures (American Public Health Association, 1998). Scavenging from carbonate species was calculated using speciation,  $k_{\bullet\text{OH},\text{CO}_3^{2-}}$  ( $8.5 \times 10^6 \text{ M}^{-1} \text{ s}^{-1}$ ) and  $k_{\bullet\text{OH},\text{HCO}_3^-}$  ( $3.9 \times 10^8 \text{ M}^{-1} \text{ s}^{-1}$ ) (Hoigne, et al., 1985). NOM was measured using a TOC-5000 (Shimadzu Corp., Japan) analyzer.

## **2.4 Results and Discussion**

### **2.4.1 Scavenging rate measurements**

Numerous methods have been developed to measure •OH scavenging in laboratory settings including competition kinetics using butyl chloride (Brezonik et al., 1998) or p-chlorobenzoic (pCBA) as a probe compound (Katsoyannis et al., 2011), experimentally defined •OH exposure dose studies ( $R_{\bullet\text{OH},\text{UV}}$ ) (Rosenfeldt et al., 2007), thiocyanate ( $\text{SCN}^-$ ) transient absorbance (Asmus, 1984), and direct measurement of radical byproduct formation (Westerhoff et al., 2007). Though effective, these methods can be time-consuming and equipment intensive because

they require high performance liquid chromatography (HPLC), gas chromatography, or high-powered  $\bullet\text{OH}$  production mechanisms such as pulse radiolysis.

To generate the number and frequency of scavenging measurements in the present research, a scavenging analysis method was needed with significantly faster throughput. Additionally, given the potential applications for in-situ scavenging measurements, a method was pursued that could be adapted to a field-deployable setup.

Herein, we developed a photometric rapid background scavenging method (R-SAM) for this purpose. The R-SAM method is based on competition kinetics, similar to what was previously described (Katsoyannis et al., 2011), however, R-SAM employs visible dyes as probe compounds that, due to their stability and high molecular absorbance, are measurable in real time without the use of high  $\bullet\text{OH}$  production rates. This modification significantly reduces the time and equipment requirements for each measurement while maintaining accuracy. R-SAM measurements can be performed in one hour and the entire R-SAM apparatus is  $0.3 \times 0.3 \times 0.3$  meters and weighs less than 5 kg. This makes the R-SAM well suited to potential field applications.

In this study, MB was employed as a probe compound, t-BuOH as the variable competitive scavenger, and UV/H<sub>2</sub>O<sub>2</sub> as the  $\bullet\text{OH}$  source; although it should be noted that a number of dye compounds and variable competitors could be substituted for MB and t-BuOH, and the results are applicable to any  $\bullet\text{OH}$  based AOP or natural  $\bullet\text{OH}$  process. The steady state hydroxyl radical equation (Equation 5) models the chemistry of the R-SAM.

$\alpha_{\bullet OH}$

$$= [\bullet OH]_{ss} (\sum_i [Scav_i] k_{\bullet OH, Scav_i} + k_{\bullet OH, t-BuOH} [t-BuOH] + k_{\bullet OH, MB} [MB] + k_{\bullet OH, H_2O_2} [H_2O_2]) \quad (5)$$

where  $\alpha_{\bullet OH}$  is the production rate of  $\bullet OH$ ,  $[\bullet OH]_{ss}$  is the steady state concentration of  $\bullet OH$ ,  $k_{\bullet OH, X}$  is the reaction rate constant of  $\bullet OH$  with a species X and  $Scav_i$  is one of i  $\bullet OH$  scavenging species present in the test water.

To perform the R-SAM analysis, solutions of MB and  $H_2O_2$  were added to the sample waters at concentrations of 1  $\mu M$  and 0.59 mM (20 mg/L), respectively. 40 ml aliquots were spiked with t-BuOH to concentrations ranging from 0 to 1,000  $\mu M$ . MB decay rates ( $k_{MB}^{app}$ ) were measured for each t-BuOH concentration with the R-SAM spectrophotometer and interpreted as in Equation (6).

$$\ln \left( \frac{abs(MB)_t}{abs(MB)_0} \right) = -k_{MB}^{app} \times t \quad (6)$$

where  $abs(MB)_t$  and  $abs(MB)_0$  are the absorbance-based concentration of MB at times t and zero respectively.  $k_{MB}^{app}$  is then used to determine  $[\bullet OH]_{ss}$  as in Equation (7) using the initial 20% of probe decay to minimize potential effects of oxidation byproducts.

$$k_{MB}^{app} = k_{\bullet OH, MB} [\bullet OH]_{ss} \quad (7)$$

Combining Eqs. 5-7 generates a relationship between  $k_{MB}^{app}$  and [t-BuOH]:

$$k_{MB}^{app} = \frac{k_{\bullet OH, MB} \times \alpha_{\bullet OH}}{\sum_i [Scav_i] k_{\bullet OH, Scav_i} + k_{\bullet OH, t-BuOH} [t-BuOH] + k_{\bullet OH, MB} [MB] + k_{\bullet OH, H_2O_2} [H_2O_2]} \quad (8)$$

$k_{MB}^{app}$  and t-BuOH concentrations were fit to Equation (8) using a least squares fit with robust regression and outlier removal (ROUT) outlier exclusion and a 5% Q value (Motulsky et al., 2006). Error was determined by propagating standard

errors from the  $k_{\text{MB}}^{\text{app}}$  measurements to generate a standard error for the first order scavenging rate measurements in  $\text{s}^{-1}$ . Confidence is reported using a T distribution with degrees of freedom = n minus two. All reported errors represent 95% confidence intervals. The detailed R-SAM procedure can be found in the Appendix.

Acknowledging the potential for interactions between water constituents and R-SAM chemicals, particularly probe dyes, the presence of such interactions was evaluated photometrically. Separate absorbance values of the MB probe and sample water at 664 nm were confirmed to be additive when combined at equivalent concentrations indicating minimal interactions between the sample water and probe compound.

The R-SAM method was validated by measuring predicted scavenging exhibited by various concentrations of IPA and t-BuOH, two scavengers with established  $k_{\text{OH}}$  rate constants (Staelin et al., 1982; Flyunt et al., 2003; Notre Dame Radiation Laboratory, 2002). The R-SAM reproduced scavenging rates predicted by the published rate constants and concentration of alcohol tested. Scavenging rate measurements were verified from 0 to  $100,000 \text{ s}^{-1}$ .

#### **2.4.2 Scavenging variability in water treatment systems**

Scavenging was measured over a period of five weeks at Plant 1 to simulate the application of AOPs for intermittent or seasonal taste and odor concerns (Figure 4). Significant variability was observed in raw river water. Coagulation-flocculation, settling and filtration lowered and stabilized scavenging levels. Interestingly, scavenging in the raw water appeared to stabilize after the initial 14 days. The scavenging data were normalized by TOC content to generate second order rate

constants for the reaction of NOM with  $\bullet\text{OH}$  ( $k_{\bullet\text{OH},\text{NOM}}$ ) (Figure 5). These data indicate a constant  $k_{\bullet\text{OH},\text{NOM}}$  in the raw ( $2.0 \pm 0.7 \times 10^8 \text{ Mc}^{-1}\text{s}^{-1}$ ) and post filtration water ( $2.0 \pm 1.0 \times 10^8 \text{ Mc}^{-1}\text{s}^{-1}$ ), when the first two samples are excluded from the raw water average.

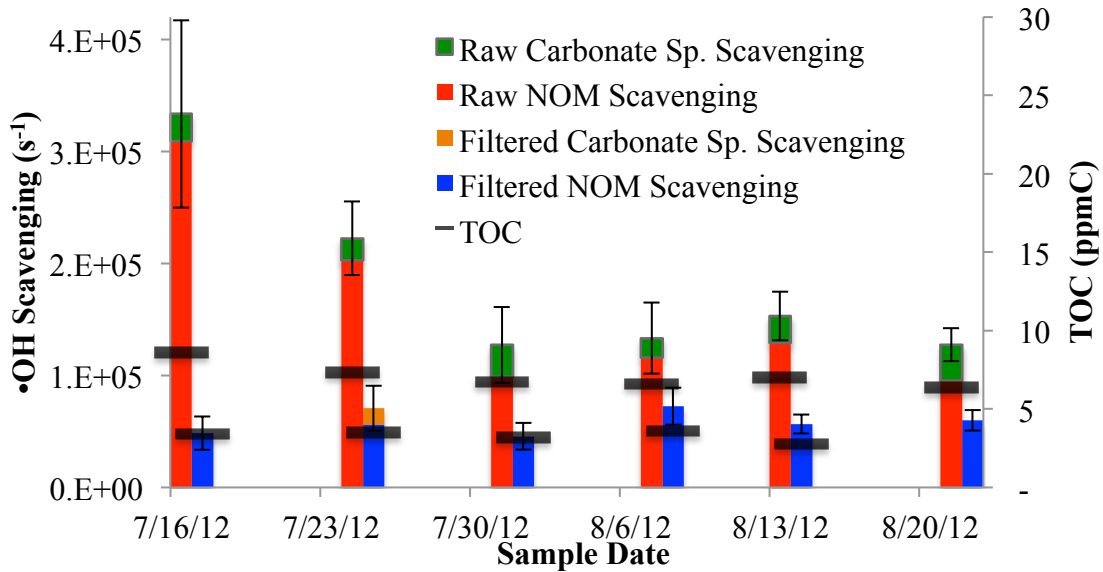


**Figure 4: Measured scavenging at lab-filtered Site 1 infulent and post-filtration water. Measured scavenging apportioned between NOM and carbonate scavenging, based on alkalinity, pH and published carbonate and bicarbonate  $\bullet\text{OH}$  reaction rate constants. TOC is also shown.**

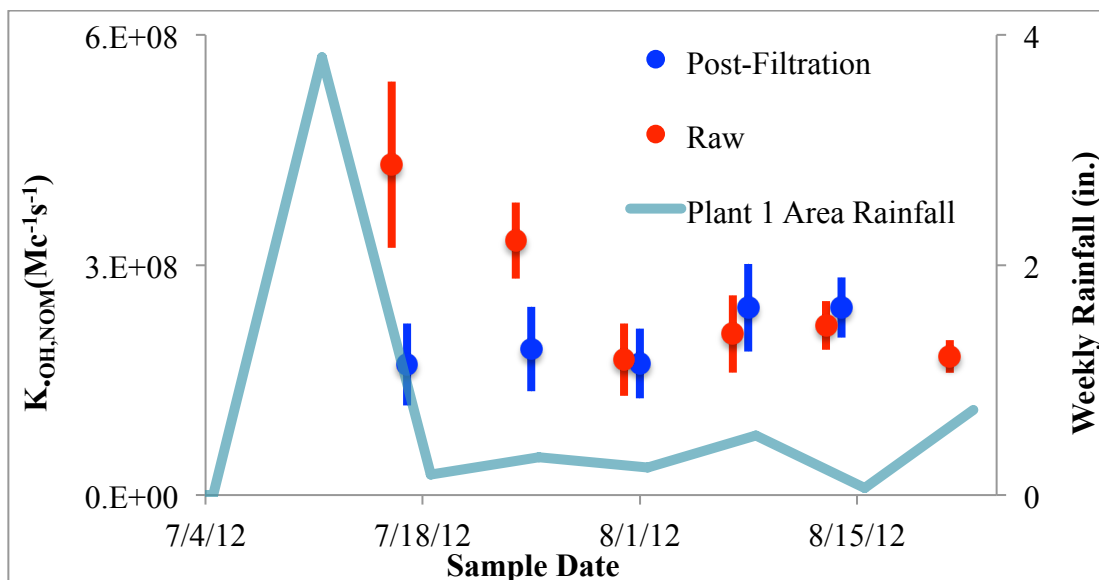


**Figure 5: Site 1 measured  $k_{OH,NOM}$  values determined by subtracting calculated carbonate scavenging and normalizing with TOC.  $k_{OH,NOM}$  (filtered) =  $2.0 \pm 1.0 \times 10^8$   $k_{OH,NOM}$  (raw, excluding first two samples) =  $2.0 \pm 0.7 \times 10^8$ .**

One possible explanation for the initial spike in bulk scavenging and NOM scavenging rate constants in the raw water is a particularly heavy rain immediately prior to the start of the sampling period. It is likely that runoff associated with the rain disturbed stratification of the large low-turbulence reservoir, or flushed in new materials. These influences may have introduced NOM of different composition, or non-carbonaceous scavengers into the Plant 1 treatment system, changing the bulk scavenging characteristics and apparent  $k_{OH,NOM}$ . An influx of non-carbonaceous scavenger, such as reduced sulfur species released when reservoir sediments are disturbed, would lead to increased scavenging levels without affecting TOC. This would lead to apparent increases in NOM rate constants in the raw water during the first two sample periods, as was observed.

Based on Plant 1 data, it is apparent that standard water treatment has significant effects on both the magnitude and variability of scavenging. Traditionally,

a strategic point for AOP implementation is the point in a treatment train where background scavenging is at a minimum to avoid scavenging demand by background material. This point is typically after filtration, but prior to final chlorination because chlorine species have been shown to have a significant scavenging effect (Jayson et al., 1973). The present results demonstrate that installing AOPs after final filtration may also be appropriate because scavenging levels are more constant at this point. Constant scavenging levels indicate reduced risk of unexpected spikes in scavenging and associated potential treatment failures.

Scavenging and NOM data were also collected over a one-year period at Plant 2 to simulate ongoing operation of an AOP to address potential trace contaminants (Figure 6 and Figure 7). Plant 2 demonstrated significant seasonal variation; scavenging rates and NOM content peaked in late fall months and were significantly higher than in late winter. Scavenging values and TOC of the filtered and unfiltered Plant 2 water were not significantly different, indicating that NOM was not filterable, and that filterable constituents did not have a large effect on scavenging rates.

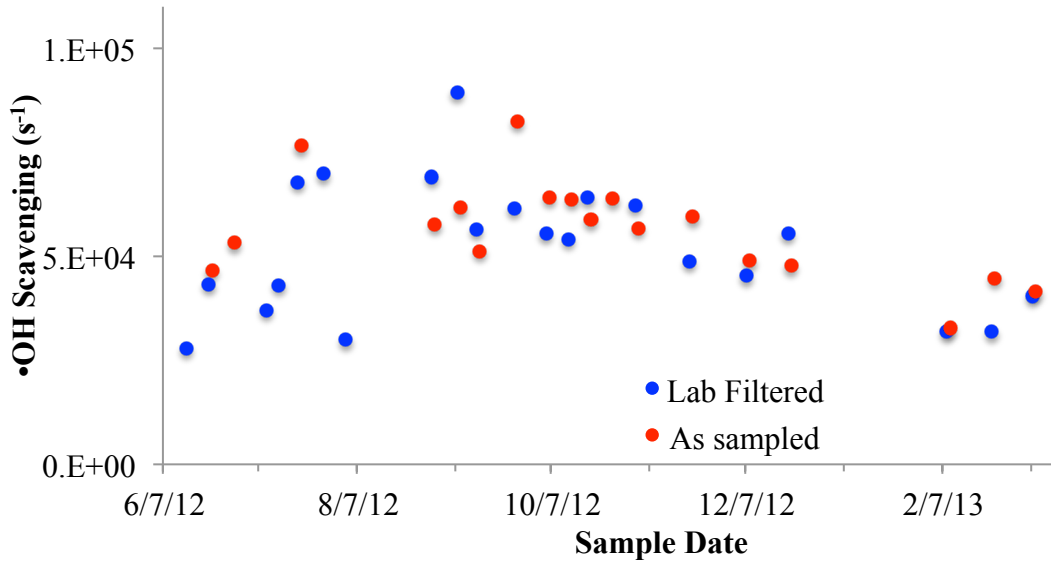


**Figure 6: Measured background scavenging in Plant 2 water post coagulation-flocculation and settling, prior to final filtration. Scavenging was evaluated in lab filtered sample water and water as sampled to gauge the effects of filterable constituents.**

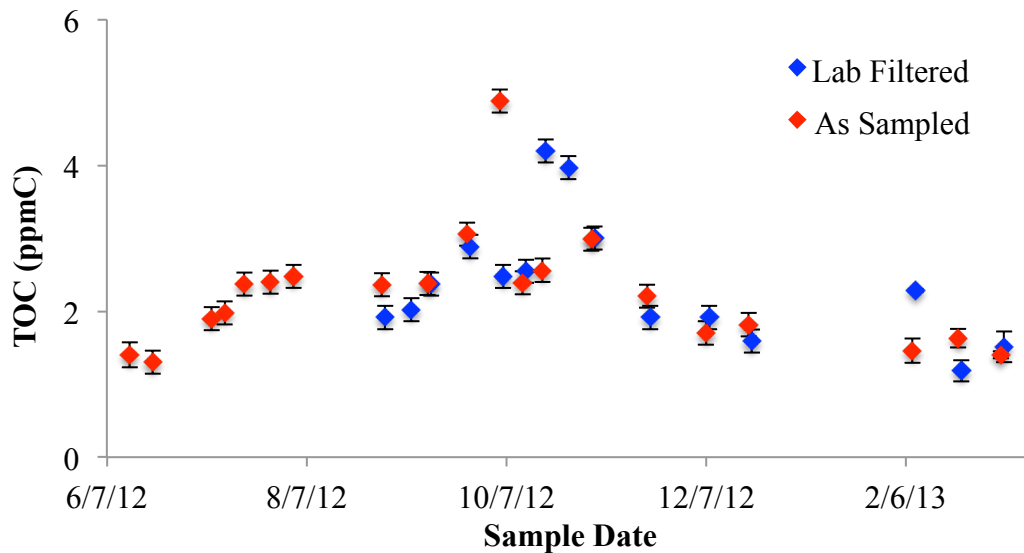


**Figure 7: Plant 2 NOM concentration in lab filtered and as sampled water.**

As before,  $k_{\text{OH},\text{NOM}}$  values were calculated for NOM present in filtered and unfiltered sample waters (Figure 8).  $k_{\text{OH},\text{NOM}}$  values at Plant 2 demonstrated significant non-systematic variability throughout the year. This finding implies that  $k_{\text{OH},\text{NOM}}$  varies considerably, irrespective of seasonality, but the majority of seasonal



variability is due to changes in NOM loading not changes in NOM composition.

Three hypotheses could explain the differences in observed variability in  $k_{\text{OH,NOM}}$  at Plant 2 as compared to Plant 1. (1) Water in the Plant 2 holding reservoir may be sensitive to short-term fluctuations in influent water quality not observed in Plant 1 due to the large dilution volumes and low velocity flow conditions of the reservoir source; (2) Plant 2 data may simply be showing that there is significantly more variability over annual cycles than over the short-term; or (3) the water composition upstream of final filtration, as was sampled at Plant 2, may not be as stable as after final filtration, as was sample at Plant 1.

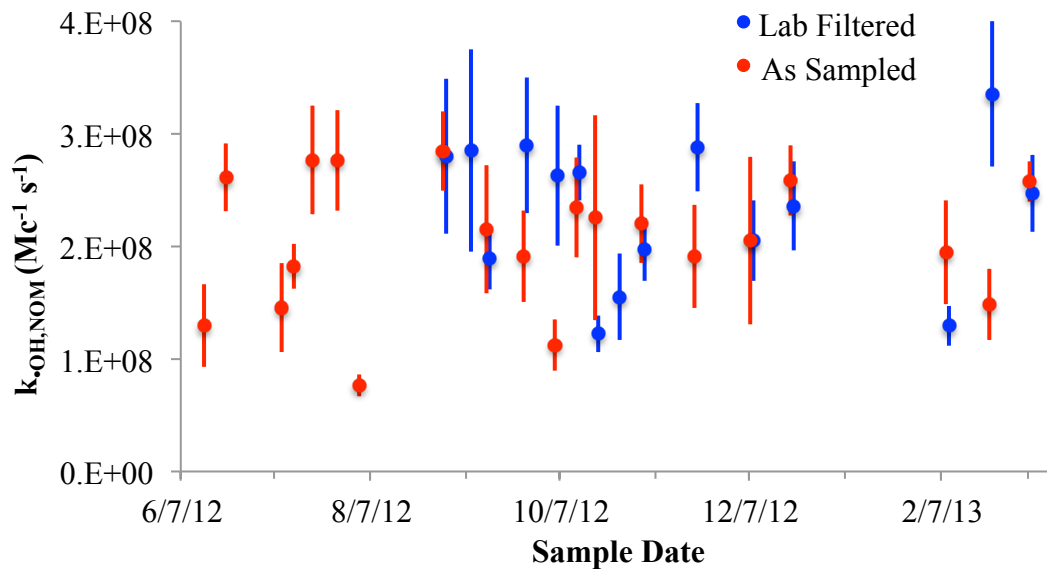


**Figure 8: Measured Plant 2  $k_{\text{OH,NOM}}$  values indicate significant variability over a factor of 3 indicating a highly variable water matrix.**

### 2.4.3 Impacts of scavenging variability on energy consumption and assurance of treatment in advanced oxidation processes

UV/H<sub>2</sub>O<sub>2</sub> AOPs, frequently used in municipal applications, provide a model to evaluate the impacts of scavenging on AOP processes applied to conventional water treatment systems, although the conclusions generated are relevant to all AOPs to some extent. To ensure constant treatment, a specific  $[\bullet\text{OH}]_{\text{ss}}$  must be maintained

through all levels of background scavenging. In UV/H<sub>2</sub>O<sub>2</sub> AOP systems, [ $\bullet$ OH]<sub>ss</sub> is proportional to scavenging, incident UV energy (I<sub>0</sub>), and H<sub>2</sub>O<sub>2</sub> concentration ([H<sub>2</sub>O<sub>2</sub>]). This can be observed in the  $\bullet$ OH production function in UV/H<sub>2</sub>O<sub>2</sub> systems (Equation 9):

$$\alpha_{\bullet OH} = \frac{I_0(1-A_{254})\epsilon_{H_2O_2}\Phi_{H_2O_2}[H_2O_2]}{U_{254}} \quad (9)$$

where,  $U_{254}$  is the energy per mole of 254 nm photons,  $A_{254}$  is the fraction of incident 254 nm photons absorbed by influent water constituents,  $\epsilon_{H_2O_2}$  is the molar extinction coefficient of hydrogen peroxide (in M<sup>-1</sup> cm<sup>-1</sup>), and  $\Phi_{H_2O_2}$  is the quantum yield of  $\bullet$ OH from hydrogen peroxide per mol of absorbed photons (Einstein or Es) (mol  $\bullet$ OH Es<sup>-1</sup>). Combining Equations (5) and (9), and simplifying yields Equation (10):

$$C \times \frac{(I_0[H_2O_2])}{(\sum_i[Scav_i]k_{\bullet OH, Scav_i} + [H_2O_2]k_{\bullet OH, H_2O_2})} = [\bullet OH]_{ss} \quad (10)$$

where C is equal to  $\frac{(1-A)\epsilon_{H_2O_2}\Phi_{H_2O_2}}{U_{254}}$  which is generally constant in a given treatment water. Holding [H<sub>2</sub>O<sub>2</sub>] constant, and dividing the general equation (10) by a specific equation (10) representative of values for a hypothetical reference case treating actual sample water demonstrates the relationship between I<sub>0</sub> and scavenging:

$$\frac{I_0}{I_{0\Box ref.}} = \frac{(\sum_i[Scav_i]k_{\bullet OH, Scav_i} + H)}{(N_{ref.} + H)} = \frac{(\sum_i[Scav_i]k_{\bullet OH, Scav_i})}{(N_{ref.} + H)} + \frac{H}{(N_{ref.} + H)} \quad (11)$$

where N<sub>ref.</sub> is the NOM scavenging of the reference sample, I<sub>0,ref.</sub> is the incident UV intensity required to generate the required [ $\bullet$ OH]<sub>ss</sub> in the reference sample, I<sub>0</sub> is the required UV intensity to generate [ $\bullet$ OH]<sub>ss</sub> in the test subject water,

and H is the constant  $H_2O_2$  scavenging rate ( $[H_2O_2] \times k_{OH,H_2O_2}$ ). Equation (11) demonstrates scavenging is directly related to the UV energy ( $I_0$ ) required to produce a constant  $[OH]_{ss}$ , when holding  $[H_2O_2]$  constant and varying UV intensity to address scavenging levels –a reasonable assumption over moderate scavenging ranges.

Based on planning estimates, annual operation and maintenance costs for a 50 MGD plant are roughly \$2M/year for a UV/ $H_2O_2$  system, or \$44,000 per MGD, if designing to a standard constant safety factor (Supporting Information: Section 2.6, Figure 10). High-throughput and potential real-time scavenging analysis using the R-SAM, however, may provide an opportunity to reduce these costs by adjusting treatment to near real-time measured scavenging levels. To evaluate the potential effect on energy consumption, Equation (11) was used to compare energy requirements of two operational strategies: a constant scavenging strategy in which scavenging is set at the 95% confidence level based on the mean and standard deviation of all scavenging measurements throughout the year; and a variable scavenging strategy in which scavenging was adjusted in real time to address the 95<sup>th</sup> percentile of each individual R-SAM measurement.

Results indicate that adjusting UV intensity in real-time based on R-SAM measurements could result in a 41% cost reduction (or savings of roughly \$820,000 per year for a 50 MGD plant) as compared to a constant scavenging assumption selected to address the 95<sup>th</sup> percentile of annual scavenging. Additionally, because the constant scavenging assumption did not address seasonal variability, setting scavenging at the 95<sup>th</sup> percentile based on a year round average may have lead to a

greater likelihood of insufficient treatment due to greater than expected scavenging (Figure 9).

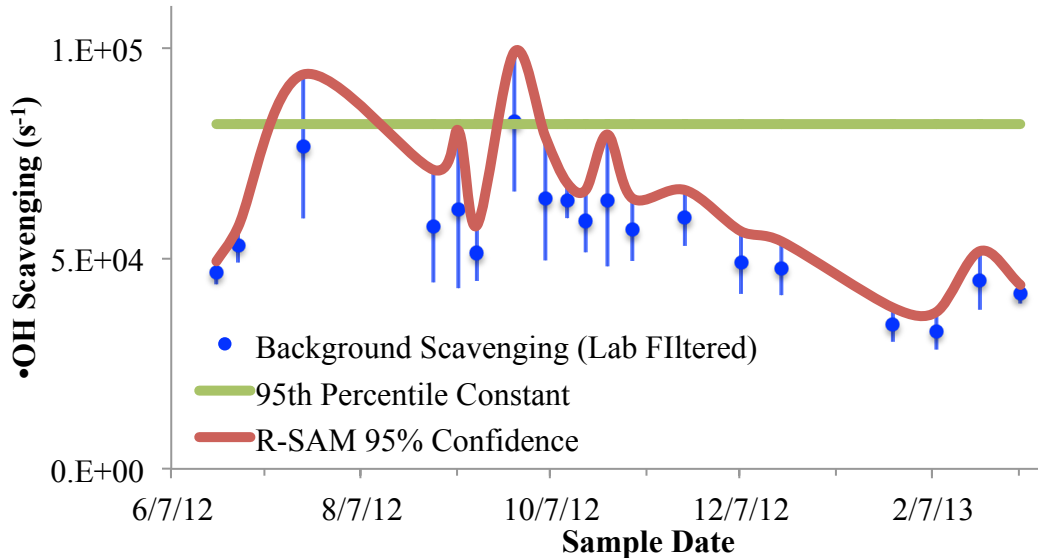


**Figure 9: NOM scavenging in Plant 2, and two operational strategies for addressing scavenging in AOP treatment: constant scavenging assumption (green), and a proposed real-time feedback strategy based on the R-SAM protocol (red).**

## 2.5 Conclusions

### 2.5.1 Scavenging variability dependent on sampling location

Plant 1, a river reservoir-fed water treatment plant, demonstrated consistent bulk scavenging rates and  $k_{\text{NOM},\text{OH}}$  rate constants after standard drinking water treatment over a period of five weeks. Interestingly, an initial spike in influent scavenging and  $k_{\text{NOM},\text{OH}}$  values, presumed to be associated with an influx of heavy rainfall runoff prior to sampling that changed the water composition, was not observed after treatment in the plant. This suggests that runoff may not affect scavenging at the preferred point of AOP application after filtration in the plant's treatment train. No runoff effects were evident in the influent three weeks after the rainfall event.

Plant 2, a directly river-fed water treatment plant, demonstrated seasonal variability in bulk scavenging levels and erratic variability in  $k_{\text{NOM},\bullet\text{OH}}$  rates at the sampling point after coagulation, flocculation and settling. This indicates that NOM loading may be responsible for the observed seasonal variability, and that  $k_{\text{NOM},\bullet\text{OH}}$  variability may be due to the shorter residence time of the Plant 2 short term influent holding reservoir as compared to the large Plant 1 influent reservoir.

Comparing Plant 1 to Plant 2 results indicate that there may be relatively consistent scavenging levels over a few weeks time, but seasonal changes may disrupt this stability on a longer time scale. Additionally, high flow-rate associated turbulence and decreased residence time of the influent body of water may decrease the stability of observed  $k_{\text{NOM},\bullet\text{OH}}$ .

### **2.5.2 The R-SAM method has applications in real-time control of AOP systems.**

Based on Site 2 sampling data, two operational strategies for addressing scavenging in AOP design and operation were evaluated for their energy consumption and reliability of treatment. Adjusting  $\bullet\text{OH}$  production rates in response to real time scavenging levels could reduce operating costs of an AOP system by roughly 41% at Plant 1 while reducing the risk of potential under treatment. This could result in a significant savings in implementing AOP technology and increased reliability of treatment.

## 2.6 Chapter 2 Supporting Information

Capacity	H <sub>2</sub> O <sub>2</sub>	Hypochlorous Acid (to quench residual H <sub>2</sub> O <sub>2</sub> )	Power	Lamp Replacement	Total O&M	Unit O&M
MGD	\$k	\$k	\$k	\$k	\$k	\$k/MGD
1	8.3	15	20	4	47	47
5	50	67	90	10	217	43
10	83	150	190	20	443	44
20	167	283	370	50	870	44
30	267	433	560	70	1,330	44
40	350	567	740	90	1,747	44
50	433	717	930	110	2,190	44
60	517	850	1,110	140	2,617	44
70	600	1,000	1,300	160	3,060	44
80	683	1,133	1,480	180	3,477	43

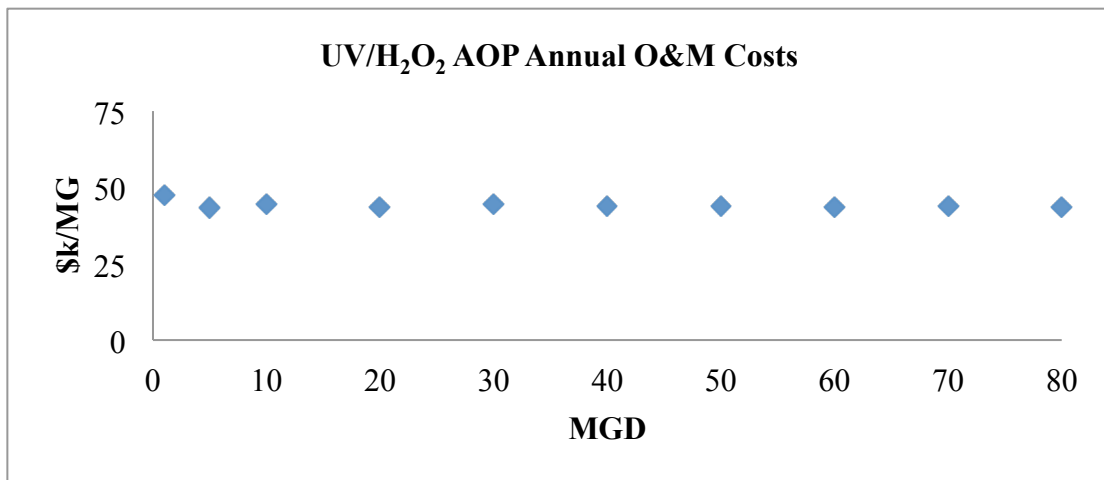


Figure 10: Municipal scale UV/H<sub>2</sub>O<sub>2</sub> operations and maintenance annual costs.

## 2.7 Chapter 2 References

American Public Health Association, American Water Works Association, and Water Environment Federation, 1998. Standard methods for the examination of water and wastewater, 20th ed.: Washington, D.C.

Asmus, K.D., 1984. Pulse Radiolysis Methodology. *Methods of Enzymology* 105, 167-178.

Banat, F., Al-Asheh, S., Al-Rawashdeh, M., Nusair, M., 2005. Photodegradation of methylene blue dye by the UV/H<sub>2</sub>O<sub>2</sub> and UV/acetone oxidation processes. *Desalination* 181 (1), 225-232.

- Bolton, J.R., Linden, K.G., 2003. Standardization of Methods for Fluence (UV Dose) Determination in Bench-Scale UV Experiments. *Journal of Environmental Engineering* 129 (3), 209-215.
- Comninellis, C., Kapalka, A., Malato, S., Parsons, S., Poullos, I., Mantzavinos, D., 2008. Advanced Oxidation Processes for Water Treatment: Advances and Trends for R&D. *Journal of Chemical Technology and Biotechnology* 83 (6), 769–776.
- Dorfman, L.M., Adams, G.E., 1973. Reactivity of the Hydroxyl Radical, National Bureau of Standards, Report No. NSRDS-NBS-46.
- EPA, 1998. Handbook on Advanced Photochemical Oxidation Processes. US Environmental Protection Agency, EPA/625/R-98/004, Cincinnati, Ohio 45266.
- Espulgas, S., Bila, D.M., Krause, L.G.T., Dexotti, M., 2007. Ozonation and Advanced Oxidation Technologies to Remove Endocrine Disrupting Chemicals (EDCs) and Pharmaceuticals and Personal Care Products (PPCPs) in Water Effluents. *Journal of Hazardous Materials* 149 631-642.
- Flyunt, R., Leitzke, A., Mark, G., Mvula, E., Reisz, E., Schick, R., von Sonntag, C., 2003. Determination of  $\bullet\text{OH}$ ,  $\text{O}_2\bullet^-$ , and hydroperoxide yields in ozone reactions in aqueous solution. *Journal of Physical Chemistry B* 107 (30), 7242-7253.
- Goldstone, J.V., Pullin, M.J., Bertilsson, S., Voelker, B.M., 2002. Reactions of hydroxyl radical with humic substances: bleaching, mineralization, and production of bioavailable carbon substrates. *Environmental Science and Technology* 36 (3), 364-372.
- Hao, X.L., Zhou, M.H., Zhang, Y., Lei, L.C., 2006. Enhanced degradation of organic pollutant 4-chlorophenol in water by non-thermal plasma process with  $\text{TiO}_2$ . *Plasma Chemistry and Plasma Process* 26 (5), 455–468.
- Hoigné, J., Bader, H., Haag, W.R., Staehelin, J., 1985. Rate constants of reactions of ozone with organic and inorganic compounds in water—III. Inorganic compounds and radicals. *Water Research*, 19 (8), 993-1004.
- Jayson, G.G., Parsons, B.J., 1973. Some simple, highly reactive, inorganic chlorine derivatives in aqueous solution. *Journal of the Chemical Society, Faraday Transactions 1: Physical Chemistry in Condensed Phases* 69, 1597–1607.
- Katsoyiannis I.A., Canonica S., von Gunten U., 2011. Efficiency and energy requirements for the transformation of organic micropollutants by ozone,  $\text{O}_3/\text{H}_2\text{O}_2$  and  $\text{UV}/\text{H}_2\text{O}_2$ . *Water Research* 45 (13), 3811-3822.
- Kolpin, D.W., Furlong E.T., Neyer, M.T., Thurman, M., Zaugg, S.D., Barber, L.B. Buston, H.T., 2002. Pharmaceuticals, hormones, and other organic wastewater contaminants in U.S. streams, 1999–2000: A national reconnaissance. *Environmental Science and Technology* 36 (6), 1202-1211.
- Lee, Y., von Gunten, U., 2010. Oxidative transformation of micropollutants during municipal wastewater treatment: comparison of kinetic aspects of selective (chlorine, chlorine dioxide, ferrate VI and ozone) and non-selective oxidants (hydroxyl radical). *Water Research* 44 (2), 555-556.

- McKay G., Dong M.M., Kleinman J.L., Mezyk M.P., Rosario-Ortiz F.L., 2011. Temperature dependence of the reaction between the hydroxyl radical and organic matter. *Environmental Science & Technology* 45 (16), 6932-6937.
- McKay, G., Kleinman, J.L., Johnston, K.M., Dong, M.M., Rosario-Ortiz, F.L., Mezyk, S.P., 2013. Kinetics of the reaction between the hydroxyl radical and organic matter standards from the International Humic Substance Society. *Journal of Soils and Sediments*, 1-7.
- Moncayo-Lasso, A., Mora-Arismendi, L.E., Rengifo-Herrera, J.A., Sanabria, J., Benitez, N., Pulgarin, C., 2012. The detrimental influence of bacteria (*E. coli*, *Shigella* and *Salmonella*) on the degradation of organic compounds (and vice versa) in TiO<sub>2</sub> photocatalysis and near-neutral photo-Fenton processes under simulated solar light. *Photochemical and Photobiological Sciences* 11 (5), 821-827.
- Motulsky, H.J., Brown R.E., 2006. Detecting outliers when fitting data with nonlinear regression—a new method based on robust nonlinear regression and the false discovery rate. *BMC bioinformatics* 7 (1) 123.
- Notre Dame Radiation Laboratory, 2002. Radiation Chemistry Data Center, Kinetics Database. [www.rccd.nd.edu](http://www.rccd.nd.edu) (accessed March 10, 2008).
- Peternel, I.T., Koprivanac N., Bozic, A.M.L., Kusic, H. M., 2007. Comparative study of UV/TiO<sub>2</sub>, UV/ZnO and photo-Fenton processes for the organic reactive dye degradation in aqueous solution. *Journal of Hazardous Materials* 148 (1), 477–484.
- Rosario-Ortiz, F.L., Mezyk, S.P., Doud, D.F., Snyder, S.A., 2008. Quantitative correlation of absolute hydroxyl radical rate constants with non-isolated effluent organic matter bulk properties in water. *Environmental Science & Technology* 42 (16), 5924-5930.
- Rosenfeldt, E.J., Linden, K.G., 2004. Degradation of endocrine disrupting chemicals bisphenol a, ethinyl estradiol, and estradiol during UV photolysis and advanced oxidation processes. *Environmental Science and Technology* 38, 5476-5483.
- Rosenfeldt, E.J., Linden, K.G., 2007. The ROH<sub>UV</sub> concept to characterize and the model UV/H<sub>2</sub>O<sub>2</sub> process in natural waters. *Environmental Science and Technology* 41, 2548-2553.
- Sharp E.L., Parsons, S.A., Jefferson, A., 2006. Seasonal variations in natural organic matter and its impact on coagulation in water treatment. *Science of the Total Environment* 363, 183–194.
- Staelin, J., Hoigné, J., 1982. Decomposition of ozone in water: rate of initiation by hydroxide ions and hydrogen peroxide. *Environmental Science and Technology* 16 (10), 676-681.
- Stumm, W., Morgan, J.J., 1996. *Aquatic Chemistry: Chemical equilibria and rates in natural waters*, third ed. Wiley INT Publication, New York.



- Trojan Technologies Inc. 2005. Trojan's UV -oxidation solutions for seasonal taste and odor. Engineering America Website. Retrieved 7/17/2013 from <[http://www.engamerica.com/uploaded/Doc/Trojan\\_Taste\\_and\\_Odor\\_Application\\_Sheet.pdf](http://www.engamerica.com/uploaded/Doc/Trojan_Taste_and_Odor_Application_Sheet.pdf)>
- Tucson Water, 2012. Advanced oxidation process (AOP) water treatment facility fact sheet. City of Tucson Arizona Website. Retrieved 7/5/2013 from <[http://cms3.tucsonaz.gov/sites/default/files/water/docs/071812\\_aop\\_facts.pdf](http://cms3.tucsonaz.gov/sites/default/files/water/docs/071812_aop_facts.pdf)>
- Weather Underground, Inc., 2013. Weather History for Fredericksburg, VA: Weeks of July 8, 2012 to August 19, 2012. wunderground.com. Retrieved 6/13/2013 from <<http://www.wunderground.com/history/airport/KEZF/2012/8/22/WeeklyHistory.html?MR=1>>.
- Westerhoff, P., Aiken, G., Amy, G., Debroux, J., 1999. Relationships between the structure of natural organic matter and its reactivity towards molecular ozone and hydroxyl radicals. *Water Research* 33 (10), 2265–2276.
- Westerhoff, P., Mezyk, S.P., Cooper, W.J., Minakata, D., 2007. Electron pulse radiolysis determination of hydroxyl radical rate constants with Suwannee River fulvic acid and other dissolved organic matter isolates. *Environmental Science and Technology* 41 (13), 4640–4646.

## Chapter 3: Photometric Hydroxyl Radical Scavenging Analysis of Standard NOM Isolates

### **3.1 Abstract**

Hydroxyl radical ( $\bullet\text{OH}$ ) scavenging reaction rate constants of standard natural organic matter (NOM) isolates ( $k_{\text{OH, NOM}}$ ) were measured to evaluate the capabilities of the rapid scavenging analysis method (R-SAM), and expand the dataset of published reaction rate constants. The R-SAM was optimized by screening for unexpected interactions between probes and NOM, and identifying a reagent mix that minimized confounding interactions. Aberrant behavior was observed in NOM-methylene blue probe compound interactions. Ultimately fluorescein was selected as an alternate  $\bullet\text{OH}$  probe and t-BuOH as the variable competitor. Rate constants for the six IHSS NOM standard isolates ranged from  $1.02 (\pm 0.23) \times 10^8 \text{ Mc}^{-1}\text{s}^{-1}$  for Suwannee River Fulvic Acid I Standard to  $2.01 (\pm 0.28) \times 10^8 \text{ Mc}^{-1}\text{s}^{-1}$  for Pony Lake Fulvic Acid Reference NOM –to 95% confidence. The reaction rate of the disodium fluorescein probe with  $\bullet\text{OH}$  ( $k_{\text{OH, Fl.}}$ ) was measured as  $1.16 (\pm 0.21) \times 10^{10} \text{ M}^{-1}\text{s}^{-1}$  for use in the optimized R-SAM method –to 95% confidence. Potential impacts of diffusion limited  $\bullet\text{OH}$  reactions and NOM-probe interactions, as well as general approaches to NOM- $\bullet\text{OH}$  kinetic models are reported. Suggestions are proposed to address these impacts in future research involving  $\bullet\text{OH}$  reaction rates.

### **3.2 Introduction**

Natural organic matter (NOM) plays a significant role in hydroxyl radical ( $\bullet\text{OH}$ ) fate in advanced oxidation processes (AOPs) for pollutant mitigation (Katsoyiannis et al., 2011), and in photochemical degradation of organic pollutants and elemental cycling in aquatic environments (Mostofa et al., 2013; McKay et al.,

2013). Even in relatively pristine waters with traces of NOM (~ 2.5 mg/L TOC), NOM can comprise more than 90% of the total demand (scavenging) of produced •OH, based on published reaction rates. Unfortunately, the relationship between NOM composition and scavenging behavior eludes a detailed understanding (Westerhoff et al, 2007). For this reason, increasing our understanding the scavenging behavior of NOM is critically important to accurately predicting or modeling •OH chemistry in natural and engineered systems.

Previous work (Brezonik et al., 1998; Goldstone et al., 2002; Westerhoff et al., 2007; McKay et al., 2011; McKay et al., 2013) investigated the role of background NOM in •OH chemistries, and demonstrated considerable variability in the reaction rate of NOM with •OH ( $k_{\text{OH, NOM}}$ ) between NOM sources. Brezonik reported reaction rate constants of NOM with •OH ranging from  $1.4 - 4.0 \times 10^8 \text{ Mc}^{-1} \text{ s}^{-1}$  for NOM present in five surface waters. Goldstone reported rate constants of  $3.2 \times 10^8 \text{ Mc}^{-1} \text{ s}^{-1}$  and  $2.28 \times 10^8 \text{ Mc}^{-1} \text{ s}^{-1}$  for Suwannee River Fulvic and Humic Acids standard isolates, respectively. Westerhoff (2007) reported a range of constants from  $1.39 - 2.18 \times 10^8 \text{ Mc}^{-1} \text{ s}^{-1}$ . McKay presented rates ranging from  $1.21 - 10.36 \times 10^8 \text{ Mc}^{-1} \text{ s}^{-1}$  for five NOM isolate standards. The wide range of NOM-•OH rate constants leads to significant uncertainties when attempting to model •OH systems given the dominance of NOM in scavenging.

To investigate possible causes of variability in NOM scavenging rates, links between NOM characteristics and scavenging rate constants have been evaluated. In particular, researchers have attempted to correlate rate constants with NOM weight averaged molecular weight (MW), carbon content, hydrogen content, nitrogen

content, oxygen content, and the ratio of aliphatic to aromatic carbon. Individually, these variables are not significantly correlated with NOM scavenging rates (McKay et al., 2013; Westerhoff et al., 2007). Rosario-Ortiz (2008), demonstrated success in developing a predictive model of NOM  $\bullet$ OH scavenging rate constants by using multivariate regression of six characteristics of a wastewater effluent organic matter (EfOM), a class of chemicals with properties similar to NOM. Correlating scavenging rates with molar weight (MW), specific UV absorbance at 254 nm ( $SUVA_{254}$ ), dispersity, hydrophobicity, anionic character, and ratio of the fluorescence emission intensities at 450 nm to 500 nm after excitation at 370 nm (a correlate of microbial versus terrestrial origins) developed a model capable of predicting scavenging rate constants within 10%. This predictive method has yielded promising results, but requires measuring numerous variables to determine scavenging rates.

Alternatively, Westerhoff (2007) modeled NOM- $\bullet$ OH reaction rates by using a weighted average of reaction rates of well-understood model compounds with  $\bullet$ OH. The model compounds were chosen to represent functional groups present in NOM and the portion of carbon in aromatic structures present in NOM isolates. Although the method was not used to predict NOM scavenging, it does pose an alternate approach to analyzing NOM. In short, the current understanding of NOM- $\bullet$ OH reactions is insufficient to support precise  $\bullet$ OH research and AOP design.

The present work employs the novel rapid  $\bullet$ OH scavenging analysis method (R-SAM) to expand the methods and knowledge available to evaluate NOM- $\bullet$ OH reactions. R-SAM is used measure the reaction rates of NOM isolate standards for

comparison with previous measurements, and to extend the dataset of published •OH scavenging rate constants for standard NOM isolates. The second order reaction rates  $k_{\bullet\text{OH}, \text{NOM}}$  ( $\text{Mc}^{-1}\text{s}^{-1}$ ) were determined for six NOM isolates from the International Humic Substances Society (IHSS) and compared to previous reports that used alternate •OH scavenging measurement techniques. Measured  $k_{\bullet\text{OH}, \text{NOM}}$  values were also evaluated with regard to nitrogen, hydrogen, carbon and oxygen elemental composition, aliphatic/aromatic carbon content, and MW to replicate work done by McKay and others (2013). Observations regarding disruptive interactions between R-SAM reagents, current approaches to predictive NOM scavenging rate modeling, and potential implications of diffusion limitations of •OH reactions were discussed to support future research.

### ***3.3 Materials and Methods***

#### **3.3.1 Chemicals**

Methylene blue (MB), hydrogen peroxide ( $\text{H}_2\text{O}_2$ ), isopropyl alcohol (IPA), tertiary butyl alcohol (t-BuOH), fluorescein disodium salt (fluorescein), and sodium hydroxide (NaOH) were obtained from Thermo Fisher Scientific Inc. (Waltham, Massachusetts) and used as received.

#### **3.3.2 Investigated isolates**

Six NOM isolates, Pony Lake Fulvic Acid Reference (cat no. 1R109F); Eliot Soil Humic Acid Standard (cat no. 1S102H); Pahokee Peat Fulvic Acid II Standard (cat no. 2S103F); Pahokee Peat Humic Acid Standard (cat no. 1S103H); Suwannee River Fulvic Acid I Standard (cat no. 1S101F); and Suwannee River Humic Acid II

Standard (cat no. 2S101H) were obtained from the International Humic Substances Society (IHSS).

NOM stock solutions were prepared by dissolving 30-60 mg of the acid standard in 0.5 L deionized water to make concentrated stock solutions NOM. The pH was adjusted to above 8.0 with NaOH before stirring the solution vigorously for one hour. The solutions were stored at room temperature for 24 hours to ensure complete dissolution, then stored at 4° C until use. All experiments were conducted within four weeks of NOM stock solution preparation. The final concentration of NOM stocks was determined with a TOC-5000 (Shimadzu Corp., Japan) analyzer (minimum detection level = 0.2 mgC/L). Standard curves included concentrations between 2,500 and 6,250  $\mu\text{Mc}$  (30 and 75 mgC/L) TOC; tested NOM concentrations were typically between 300 and 500  $\mu\text{Mc}$ .

### **3.3.3 R-SAM equipment**

Scavenging measurements were made with a photometric R-SAM process, as described previously (Hross, 2010). In brief, R-SAM employs competition kinetics using a high absorbance dye as a  $\bullet\text{OH}$  probe compound. Apparent reaction rates of the probe dye with  $\bullet\text{OH}$  are measured in sample water with varying concentrations of a competitive scavenger to determine the first-order scavenging rate of the sample water (in  $\text{s}^{-1}$ ). The first-order scavenging rate is then divided by the NOM concentration (Mc) of the sample to report a second order rate constant for the reaction of  $\bullet\text{OH}$  with the sample NOM ( $k_{\bullet\text{OH}, \text{NOM}}$  in  $\text{Mc}^{-1}\text{s}^{-1}$ ). Error was propagated from the independent errors of TOC measurement and R-SAM calculations. A T-

distribution with degrees of freedom equal to the number of independent runs in the initial R-SAM regression minus two was used to generate 95% confidence intervals.

Some modifications had to be made to the R-SAM procedure to facilitate NOM analysis. NOM isolates absorb throughout the UV-Vis spectrum causing NOM absorbance to overlap with the absorbance spectra of the two tested probes (MB and fluorescein) (Figure 11). To address this problem, an NOM sample (at the concentration to be tested) was used as the 100% transmittance blank. This allowed accurate measurement of probe absorbance, concentration and degradation rate without confounding NOM absorbance at relevant wavelengths. To validate this correction, it was confirmed that the NOM absorbance baseline did not change (bleach) at the wavelengths used to track probe decay when the solution was exposed to UV. NOM bleaching would artificially increase the measured degradation rate of the dye when used as the blank. Resistance to photo bleaching of NOM in the R-SAM reactor was monitored over five minutes of exposure (longer than standard R-SAM test runs). Observed bleaching was less than 1%. This confirmed a constant baseline absorbance.

### ***3.4 Results***

#### **3.4.1 Selection of probe compound and optimization of NOM scavenging measurement method**

To be suitable for R-SAM analysis of a specific water matrix, a probe compound must meet multiple criteria: (1) have high molar absorptivity; (2) be insensitive to pH changes in the neutral range (pH from 5 - 9); (3) produce no reactive byproducts after  $\bullet\text{OH}$  oxidation; (4) have an established second order reaction rate with  $\bullet\text{OH}$  for use in the R-SAM equation (12):

$$k_{Probe}^{app} = \frac{k_{\bullet OH, Probe} \times \alpha_{\bullet OH}}{\sum_i [Scav_i] k_{\bullet OH, Scav_i} + k_{\bullet OH, VC} [VC] + k_{\bullet OH, Probe} [Probe] + k_{\bullet OH, H_2O_2} [H_2O_2]} \quad (12)$$

where  $\alpha_{\bullet OH}$  is the steady state production rate of  $\bullet OH$ ,  $k_{probe}^{app}$  is the measured degradation rate of the probe,  $Scav_i$  refers to one of  $i$  scavenging species in solution, and VC represents a variable competitor; (5) resist decay under  $UV_{254}$  exposure; and (6) be inert with regard to sample constituents (predominantly NOM in the present work) and the variable competitor.

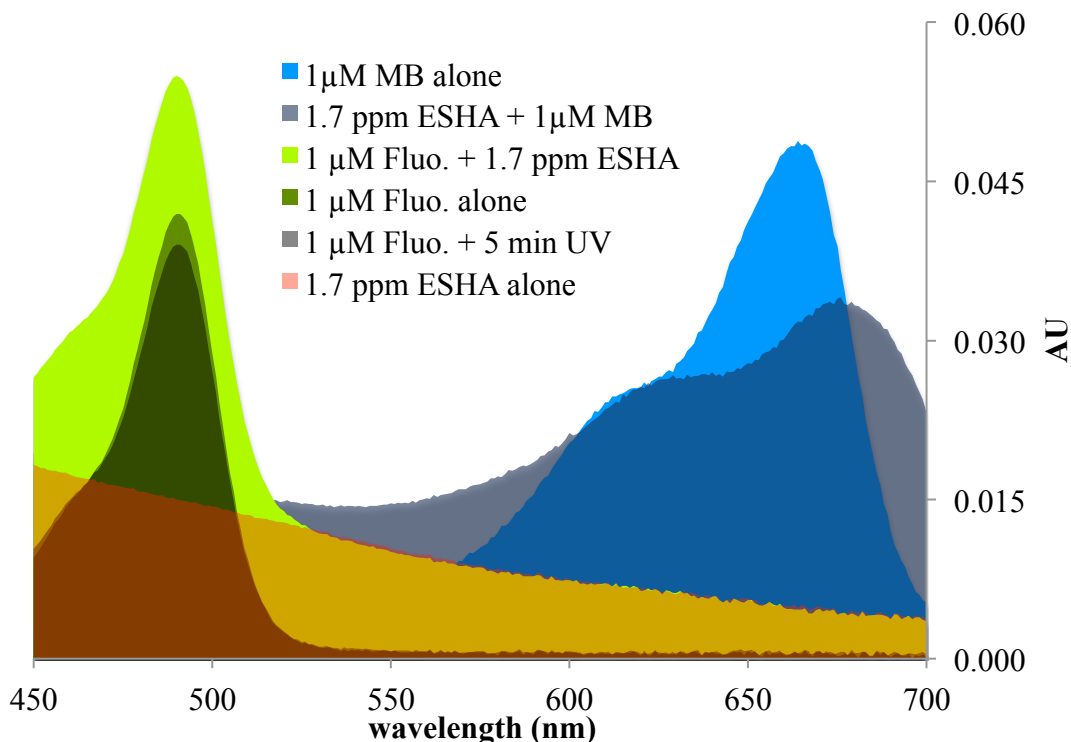
MB has been used successfully as a probe dye in the R-SAM method for measuring scavenging in drinking water (Chapter 2). Per criteria (1 and 2) MB has a high molar absorptivity ( $6.9 \times 10^4 \text{ M}^{-1}\text{cm}^{-1}$ ; Prahl, 2013), and low  $pK_a$  ( $< 1$ ) indicating general pH insensitivity (The United States Pharmacopeial Convention, 2008).

With respect to criterion 3, MB demonstrated consistent second order behavior over a wide range (80%) of decay (supporting information, section 3.7, Figure 13). Per criterion 4, the reaction rate for MB with  $\bullet OH$  ( $1.2 \times 10^{10} \text{ M}^{-1}\text{s}^{-1}$ ) was available in the literature (Banat et al., 2005). Per criterion 5, MB did not undergo UV decay after 300 mJ/cm  $UV_{254}$  in 1  $\mu\text{M}$  MB (.32 mg/L) (supporting information, section 3.7, Figure 13); for comparison, the maximum exposure in typical R-SAM measurements is 9 mJ/cm. Per criterion (6) it was confirmed that MB was inert in the presence of the sample water by verifying that absorbances were additive (Figure 11).

In the presence of concentrated NOM isolates, however, the absorbance values of NOM and MB were not additive at 664 nm (the wavelength selected for the R-SAM MB analysis). Upon addition of 1.7 mg/L ESHA to a 2  $\mu\text{M}$  (0.64 mg/L) solution of MB, absorbance decreased by a factor of two (Figure 11). It was therefore



concluded that MB interacted with the NOM and was thus deemed a non-ideal probe compound for measuring  $\bullet\text{OH}$  scavenging in NOM isolates.

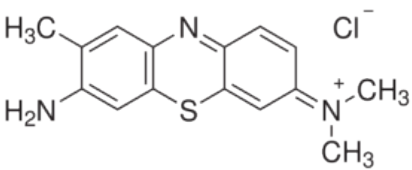
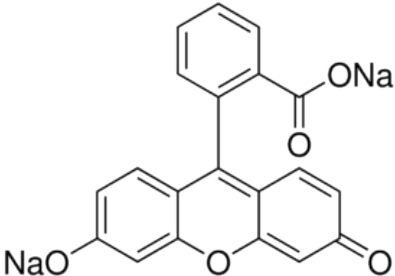


**Figure 11: NOM adsorption and UV decay in methylene blue and fluorescein**

The non-additive absorbance of MB and NOM isolate standards was determined to be due to attractions between the positively charged MB ion (Table 1) and NOM isolate standards composed of negatively charged humic acid material. Although MB may be appropriate for other R-SAM applications, it is deemed inappropriate for samples with high concentrations of humic acid.

A second probe compound, fluorescein, was also tested. Fluorescein has previously been used in similar applications (Ou et al., 2002) in which fluorescein degradation rates were measured in the presence of various food-based antioxidants to determine their ability to suppress  $[\bullet\text{OH}]_{\text{ss}}$  and subsequent ability to prevent oxidative damage in living tissues. Again the six R-SAM suitability criteria were

evaluated. Regarding criterion 1 fluorescein has high molar absorptivity. Regarding criterion 2, however, fluorescein is sensitive to pH, thus absorbance was measured at the 460 nm isosbestic (pH independent) wavelength and pH maintained at least two pH units above the pKa<sub>2</sub> of fluorescein (pKa<sub>2</sub> = 6.4) with 1 M NaOH to ensure consistent deprotonation. Per criterion 3, fluorescein exhibited consistent second order behavior over a wide range (80%) of decay (supporting info, section 3.7, Figure 14).

Name	Structure	k <sub>OH</sub> (M <sup>-1</sup> s <sup>-1</sup> )	pKa
<b>Methylene Blue</b>		$1.2 \times 10^{10}$	<1
<b>Sodium Fluorescein</b>		$1.16 \pm 0.21 \times 10^{10}$	6.4

**Table 1: Methylene blue and sodium fluorescein probe dye structures (Sigma Aldrich Co. LLC, 2013) and other parameters.**

Regarding criterion 4, the reaction rate constant of fluorescein with •OH, the rate was calculated as  $1.16 \pm 0.21 \times 10^{10} \text{ M}^{-1}\text{s}^{-1}$  using methods adapted from (Rosenfeldt et al., 2004). This is in general agreement of the value reported by Cordier and others (1968) of  $1.4 \pm 0.2 \times 10^{10} \text{ M}^{-1}\text{s}^{-1}$ . Rosenfeldt's method is similar to the R-SAM method, however the degradation rate of the subject compound (e.g. fluorescein) can be directly measured instead of relying on a probe competitor, simplifying analysis. A relationship is created between the apparent degradation rate and concentration of a variable competitor allowing determination of the rate

constant. *t*-BuOH was substituted for IPA as the variable competitor in the interest of using slower reacting compounds to reduce potential diffusion limitation effects. Additionally a non-linear fit of the steady state  $\bullet\text{OH}$  formula was used instead of the reciprocal linearization previously used.

Per criterion 5, the resistance of fluorescein to direct UV photolysis by  $\text{UV}_{254}$  at doses used in the R-SAM was assessed by exposing a 1  $\mu\text{M}$  fluorescein solution to  $\text{UV}_{254}$  radiation for 5 min in the R-SAM apparatus –R-SAM analyses typically involve less than 5 minutes of exposure. After 5 minutes of exposure, less than 1% degradation was observed at 460nm –the decreased absorbance at the 494 nm peak was presumably due to pH fluctuation (Figure 11).

Regarding criterion 6, due to the negative ionic charge of fluorescein in neutral solution, less interaction with the NOM was expected. Indeed, the fluorescein and NOM absorbance values were additive at 460 nm (Figure 11), suggesting minimal interaction.

### **3.4.2 Rate constants for reaction of $\bullet\text{OH}$ with NOM isolates**

The measured rate constants for the reactions between NOM and  $\bullet\text{OH}$  ranged from 1.02 -  $2.01 \times 10^8 \text{ Mc}^{-1}\text{s}^{-1}$  (Figure 12 and Table 3), with Pony Lake Fulvic Acid Reference being the largest and Suwanee River Fulvic Acid Standard I being the smallest. The sample set included three fulvic acids and three humic acids. Results were consistent with some previous work (Westerhoff et al., 2007), but significantly different than other work (McKay et al., 2011; McKay et al., 2013) (Figure 12). Interestingly, R-SAM results for SRHA II-S were consistent with some results for

SRHA I-1 from (Westerhoff et al., 2007). SRHA I-S and SRHA II-S are from the same source, but sampled in 1982-1983 and 2003 respectively.

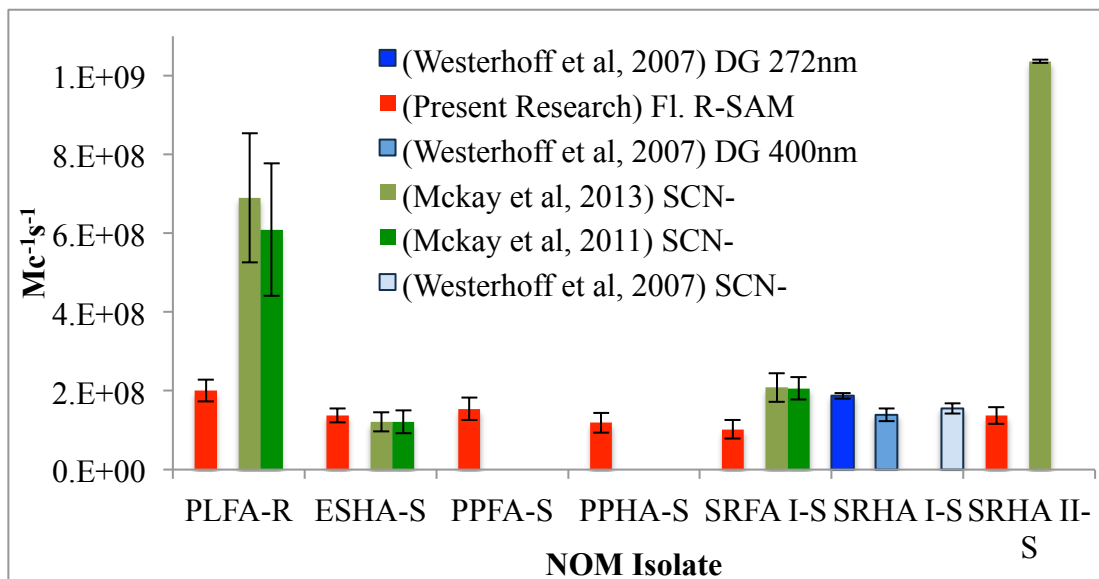


**Figure 12: Measured rate constants for NOM isolates by researcher and measurement method; Fl. R-SAM: fluorescein based R-SAM, MB R-SAM: methylene blue R-SAM, SCN-: thiocyanate competition kinetics, DG 400/272: direct measurement of transient DOM radicals at 272 and 400 nm. 95% confidence interval shown.**

IHSS Catalogue Number	NOM Name	NOM Acronym	Measured Scavenging ( $\times 10^8$ , 95% CI)
1R109F	Pony Lake Fulvic Acid Reference	PLFA-R	2.01±0.28
1S102H	Elliot Soil Humic Acid Standard	ESHA-S	1.37±0.17
2S103F	Pahoee Peat Fulvic Acid Standard (Sample Date 2)	PPFA II-S	1.54±0.28
1S103H	Pahoee Peat Humic Acid Standard (Sample Date 1)	PPHA I-S	1.19±0.25
1S101F	Suwannee River Fulvic Acid Standard (Sample Date 1)	SRFA I-S	1.02±0.23
2S101H	Suwannee River Humic Acid Standard (Sample Date 2)	SRHA II-S	1.37±0.22

**Table 2: NOM isolates studied.**

### 3.5 Discussion

#### 3.5.1 Comparison with previous results

R-SAM results for ESHA-S were consistent with previous reports but were significantly lower than previously published values for PLFA-R and SRFA I-S SRHA II-S (McKay et al., 2011; McKay et al., 2013). The range of results for NOM- $\bullet$ OH scavenging rates is in agreement with other work (Brezonik et al. 1998; Goldstone et al., 2002, Westerhoff et al., 1999; Westerhoff et al., 2007), however, McKay and associates demonstrated a considerably greater range of scavenging rate constants using methods similar to Westerhoff and others (2007). The origin of the discrepancy is unknown.

Previous work was performed using the transient thiocyanate absorbance method (SCN-) (Westerhoff et al., 2007; McKay et al., 2011; McKay et al., 2013). Similar to the R-SAM method, the oxidation of SCN- into  $\bullet(\text{SCN})_2^-$  is monitored photometrically in the presence of different concentrations of a variable competitor (in this case variable concentrations of SCN- itself). Unlike the R-SAM method, in the SCN- method, the oxidation product  $\bullet(\text{SCN})_2^-$ , not the reactant, is the optically detectable species.  $\bullet(\text{SCN})_2^-$ , however is an unstable, transient species, and must be measured with high precision equipment and analytical methods. The SCN- method also benefits from the use of a high  $\bullet$ OH production rate, such as that available from pulse radiolysis of water, to generate large quantities of  $\bullet(\text{SCN})_2^-$  quickly in an effort to minimize the effects of the rapid degradation of the  $\bullet(\text{SCN})_2^-$  product and subsequent effect on measurable concentration of  $\bullet(\text{SCN})_2^-$  (Westerhoff et al., 2007; McKay et al., 2011; McKay et al., 2013).

Alternatively, Westerhoff (2007) experimented with new methods of •OH-NOM reaction rate constant measurements by measuring the direct growth (DG) of NOM oxidation byproducts. This was performed by monitoring transient absorbance at both 272 and 400 nm. As with the SCN- method, however, the products of NOM oxidation are unstable transient species at low concentrations. DG methods therefore also benefit from high precision analytical techniques, and the use of radiolysis as a •OH source. The R-SAM method was developed to be faster and less equipment intensive than these methods and demonstrated comparable results.

### **3.5.2 Correlation of $k_{\bullet\text{OH}, \text{NOM}}$ with NOM characteristics**

Previous research has attempted to develop predictive relationships between bulk NOM properties and •OH scavenging rate constants. Similar to previous work (McKay et al., 2013; Westerhoff et al., 2007), the scavenging rate constants measured with R-SAM resulted in no significant correlation to bulk characteristics including weight averaged molecular weight [obtained from (McKay et al., (2013))], carbon content, hydrogen content, nitrogen content, oxygen content [obtained from (IHSS, 2013<sup>b</sup>)], ratio of aliphatic to aromatic carbon [obtained from (Thorn et al., 1989)] (supporting info, section 3.7, Figure 15). The small sample size, limited variability of bulk NOM characteristics, and outlying behavior of PLFA made it impossible to develop a significant relationship between bulk NOM characteristics and scavenging rates that did not rely solely on the PLFA outlier to demonstrate a correlation. Such single point correlations have been shown previously (Westerhoff et al., 1999) but reliance on a single outlier biases conclusions and should not be used to infer causal relationships (Westerhoff et al., 2007).

Pony Lake Fulvic Acid reference had the highest scavenging rate constant, and provides anecdotal insight into NOM scavenging properties. Pony Lake Fulvic Acid was isolated from a saline coastal pond in Antarctica –as compared to the temperate fresh water sources for the other isolates. Pony Lake NOM is entirely derived from microbial byproducts due to the lack of vegetation and animal life in the area (IHSS, 2013<sup>a</sup>). These unique circumstances garner high nitrogen content and low aromaticity compared with other NOM isolates. Pony Lake NOM exhibited the highest scavenging rate constant in the present work, and a higher rate in McKay and associates' work (2011; 2013). However, because many of its characteristics are strikingly different from all other isolates, it is difficult to relate the high scavenging rate constant of PLFA-R to a specific variable. Interestingly, high nitrogen content has not previously been associated with elevated •OH scavenging rate constants (McKay, 2013). And, aromaticity, as measured by SUVA<sub>254</sub>, has been shown to have a positive correlation with scavenging rate constant in multivariate analysis (Rosario-Ortiz, 2008). This positive correlation is counter to the relationship demonstrated by PLFA-R as compared to the other isolates in the present work indicating an overriding influence from another variable. Ultimately, the reason for the increased scavenging rate of PLFA-R as compared to the other isolates is unknown.

It is possible that with additional data, a multivariate approach could yield significant relationships between NOM variables and scavenging rates, as was done for EfOM isolates (Rosario-Ortiz, 2008). Alternatively, a revised interpretation of bulk NOM characteristics may help develop scavenging rate constant models that are more descriptive and thus better able to predict scavenging rate constants. Most

research has modeled NOM variables that may influence scavenging behavior as single numbers. This approach overlooks how variables might be expressed on the molecular level.

Take, for example, weight averaged MW (McKay et al., 2013). Given that reactions occur on the molecular level, the number of molecules of NOM (as defined by the mass content of NOM and molecular weight) is a crucial variable. When applying a weight averaged MW, the number of small molecules will be underestimated and grossly inaccurate. Hence, weight averaged MW does not reflect the actual number of molecules present. Using this interpretation, it is understandable why there is no evident relationship between weight averaged MW and reaction rate constants –without addressing the spread or distribution of a variable such as MW on the molecular level, the true effect of this variable may be impossible to discern.

One method of addressing the variability NOM composition within a specific isolate involves NOM fractionation. Emerging NOM fractionation methods separate NOM isolates into more homogenous groups prior to analysis based on its properties of interest (e.g. MW). Once fractionated bulk measurements of NOM properties are more reflective of all NOM present, not simply the central tendency of the sample as a whole (Dong et al., 2010). Alternatively, it is possible that by analyzing NOM characteristics as mathematical distributions of each relevant variable, instead of single aggregate values when correlating reaction rates with NOM properties, predictive rate models would more accurately address the diversity of NOM and the array of scavenging rates factors present. In the near term, given the lack of reliable NOM scavenging prediction methods, the portability and optimization of the R-SAM



method to measure NOM isolates demonstrates its potential to serve the purposes of scavenging prediction by measuring near real time, or potentially, *in situ* scavenging levels for many applications.

### **3.5.3 Implications of transport limits on fast reactions for competition kinetics based scavenging analysis**

Another cause cited for the absence of a correlation between NOM characteristics and  $k_{\bullet\text{OH},\text{NOM}}$  is the effects of diffusion or more generally transport limitations in  $\bullet\text{OH}$  reactions (von Gunten et al., 2003; Westerhoff et al., 2007). While transport limits may affect  $\bullet\text{OH}$ -NOM reactions, given the faster reaction rates of common probe compounds and variable competitors (Table 3), transport limitations may be more likely to affect these reactions that are used to determine NOM- $\bullet\text{OH}$  reaction rates to begin with. To ensure the validity of  $\bullet\text{OH}$  reaction rate constant measurements, it is important to consider how transport bounds on  $\bullet\text{OH}$  reaction rates with probes and competitors may affect conclusions regarding  $\bullet\text{OH}$  scavenging rates. Transport limitations may lead to increased sensitivity to temperature and mixing conditions causing increased error and variability in measurements, as well as potential non-first order relationships with concentration, for reactions involving those species.

In general kinetics, the rate-limiting step in chemical reactions involves the energetics of the interactions between the reacting species. The physical transportation of the species by diffusion is fast enough as to be insignificant in comparison. At fast reaction rates involving  $\bullet\text{OH}$  (i.e.  $5 \times 10^8 \text{ s}^{-1}$ ) the transport step is the rate determining step (Westerhoff et al., 2007) and at rates as slow as  $5 \times 10^7 \text{ s}^{-1}$  diffusion may be affecting rates by as much as 10%. Under such conditions,

temperature and mixing that affect diffusion rates begin to impact the apparent kinetics. Additionally, concentration, which affects the distance species must travel to react, can impact the extent to which diffusion rates govern general reaction rates (Buxton et al., 1988). The end result of these interactions is increased error associated with variability in mixing and thermal conditions, and increased apparent scavenging at low concentrations where diffusion limitations may be falsely interpreted as increased background •OH demand.

Constant	Value	Source
$k_{\bullet\text{OH}, \text{NOM}}$	$1\text{-}2 \times 10^8 \text{ M}^{-1}\text{s}^{-1}$	(Present Publication)
$k_{\bullet\text{OH}, \text{SCN}^-}$	$1.05 \times 10^{10} \text{ M}^{-1}\text{s}^{-1}$	(McKay et al., 2013)
$k_{\bullet\text{OH}, \text{MB}}$	$1.2 \times 10^{10} \text{ M}^{-1}\text{s}^{-1}$	(Banat, et al., 2005)
$k_{\bullet\text{OH}, \text{Fl.}}$	$1.2 \times 10^{10} \text{ M}^{-1}\text{s}^{-1}$	(Present Publication)
$k_{\bullet\text{OH}, \text{IPA}}$	$1.9 \times 10^{10} \text{ M}^{-1}\text{s}^{-1}$	(Rosenfeldt, 2004)
$k_{\bullet\text{OH}, \text{t-BuOH}}$	$6 \times 10^8 \text{ M}^{-1}\text{s}^{-1}$	(Stachelin et al., 1982; Flyunt et al., 2003)
$k_{\bullet\text{OH}, \text{PCBA}}$	$5 \times 10^9 \text{ M}^{-1}\text{s}^{-1}$	(Katsoyiannis et al., 2011)

**Table 3: Reaction rates constants of compounds used in competition kinetics based scavenging analyses.**

Future work should examine the impact of transport limitations on competition kinetics based •OH scavenging measurements. The experiments should characterize the effects that stirring rates have on the calculated  $k_{\bullet\text{OH}}$  values, and confirm that probes, variable competitors and scavengers follow first order kinetics across a relevant range of concentrations at various concentrations of •OH, temperatures and mixing conditions.

### 3.6 Conclusions

The R-SAM accurately reproduced published measurements of the •OH scavenging rate constant for ESHA-S but results were strikingly different than previous work for PLFA-R and SRHA II-S (McKay et al., 2011; McKay et al., 2013).

The range of all R-SAM results, however, is in general agreement with other available literature. Additionally no statistically significant relationships were evident when correlating scavenging rates with weight averaged molecular weight, carbon content, hydrogen content, nitrogen content, oxygen content, or ratio of aliphatic to aromatic carbon as was shown by Westerhoff and others (2007) and McKay and others (2013). It is proposed here, that a scheme may be developed that amends the current model of NOM scavenging behavior as a function of single-value bulk characteristics, to a model that addresses the distribution of a characteristic among molecules present in a particular NOM either analytically or using physical fractioning of NOM isolates.

Observed interactions between R-SAM reagents and subject compounds, and suspected transport limitations may affect R-SAM and other competition kinetics based  $\bullet\text{OH}$  scavenging rate constant measurement methods. To avoid such errors, future work should verify expected behaviors of probes, variable competitors and subject compounds with respect to concentration, stirring, temperature, extent of degradation and pair interactions wherever possible.

Finally, it is offered that the R-SAM significantly reduces complications involving direct scavenging measurement, and thus may supplant the need to predict scavenging in some applications.

### 3.7 Chapter 3 Supporting Information

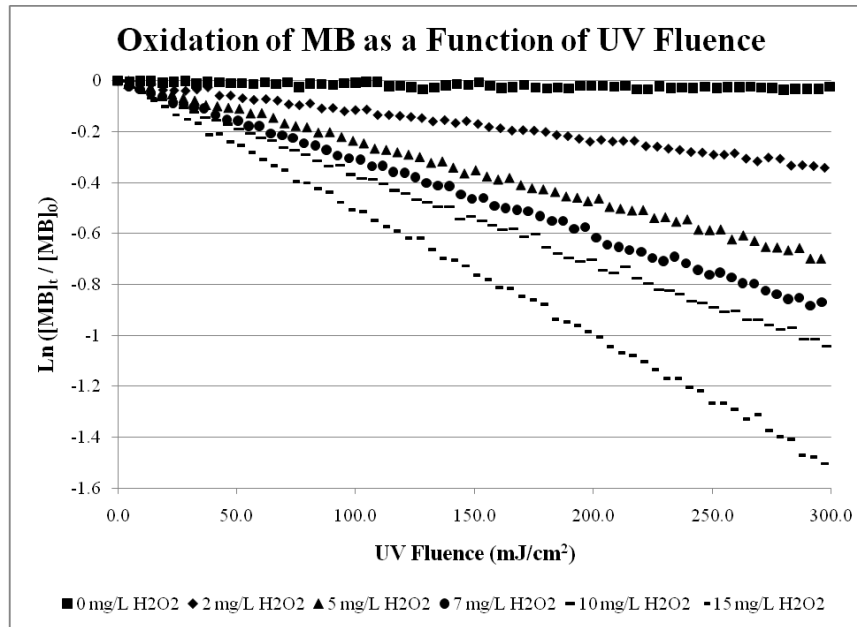


**Figure 13: Consistant second order degradation of MB to 80% decay. Minimal photodecay (at 0 mg/L H<sub>2</sub>O<sub>2</sub>) indicates resistance to UV<sub>254</sub>. Linear decay curves at higher H<sub>2</sub>O<sub>2</sub> concentrations indicates predicatable second order behavior when reacting with •OH, and limited generation of •OH scavenging byproducts.**

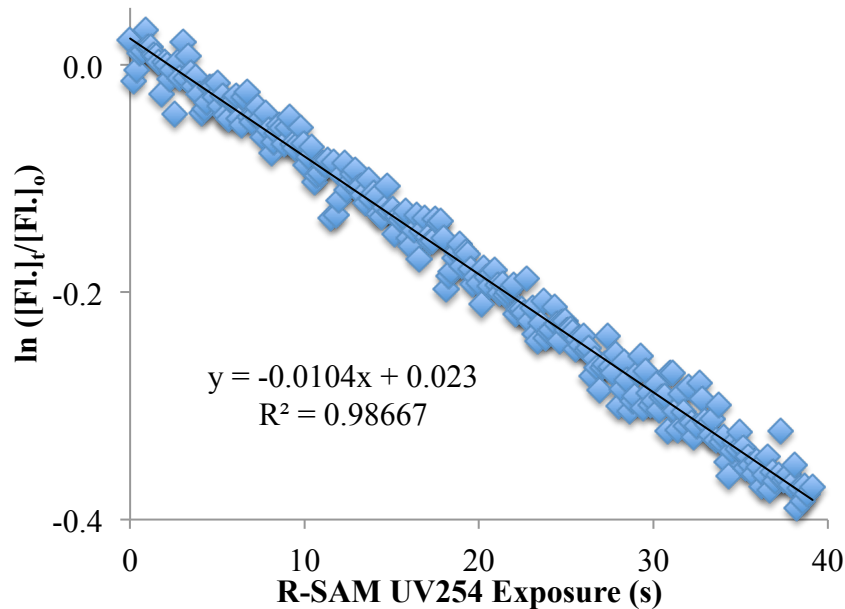


**Figure 14: Consistant second order degradation of fluorescein (FL) to 30% decay. Indicates predicatable second order behavior when reacting with •OH, and limited generation of •OH scavenging byproducts.**

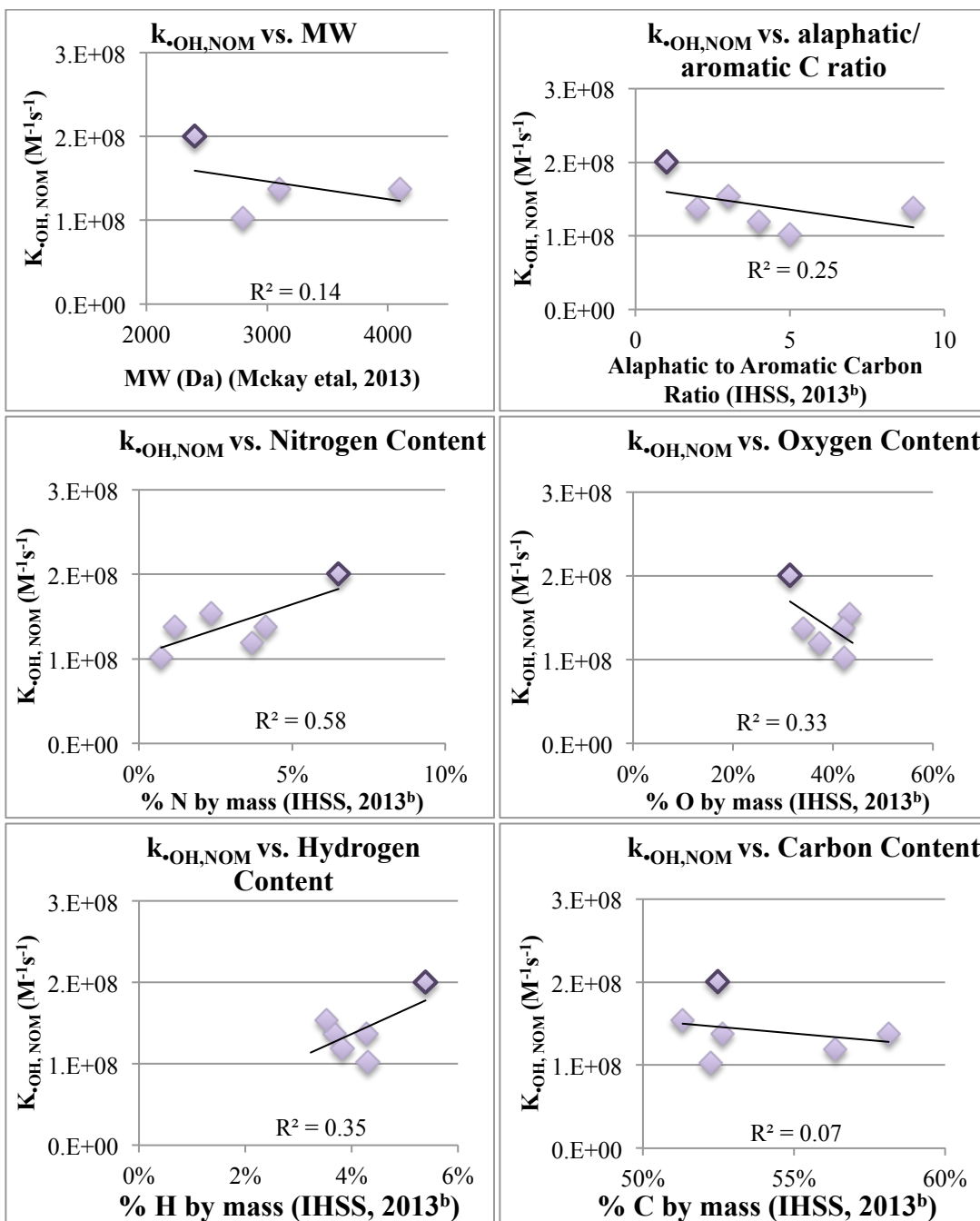


**Figure 15: Correlation of NOM characteristics with  $\bullet\text{OH}$  scavenging rate constants.  $\blacklozenge$ : PLFA-R NOM. In most cases any apparent relationship between the NOM characteristic shown and the Molar-carbon  $\bullet\text{OH}$  scavenging rate was only due to inclusion of the PLFA-R outlier.**

### 3.8 Chapter 3 References

- Banat, F., Al-Asheh, S., Al-Rawashdeh, M., Nusair, M., 2005. Photodegradation of methylene blue dye by the UV/H<sub>2</sub>O<sub>2</sub> and UV/acetone oxidation processes. *Desalination* 181 (1), 225-232.
- Buxton, G.V., Greenstock, C.L., Helman, W.P., Ross, A.B., 1988. Critical review of rate constants for reactions of hydrated electrons, hydrogen atom and hydroxyl radicals ( $\bullet\text{OH}/\bullet\text{O}$ ) in aqueous solutions. *Journal of Physical Chemistry Reference Data* 17, 513–886.
- Cordier, P., Grossweiner, L.I., 1968) Pulse radiolysis of aqueous fluorescein. *Journal of Physical Chemistry*. 72(6) 2018-2026.
- Dong, M.M., Mezyk, S.P., Rosario-Ortiz, F.L., 2010. Reactivity of effluent organic matter (EfOM) with hydroxyl radical as a function of molecular weight. *Environmental Science and Technology*, 44, 5714–5720.
- Goldstone, J.V., Pullin, M.J., Bertilsson, S., Voelker, B.M., 2002. Reactions of hydroxyl radical with humic substances: bleaching, mineralization, and production of bioavailable carbon substrates. *Environmental Science and Technology* 36 (3), 364-372.
- Hross, M.H., 2010. Rapid measurement of background hydroxyl radical scavenging in water: Masters Project. University of Massachusetts – Amherst, Department of Civil and Environmental Engineering.
- IHHS 2013.<sup>a</sup> Pony Lake Fulvic Acid: A microbially-derived fulvic acid collected from a hypereutrophic coastal pond in Antarctica. International Humic Substances Society Website. Retrieved 6/26/2013 from <<http://www.humicsubstances.org/elements.html>>.
- IHHS 2013.<sup>b</sup> Elemental Compositions and Stable Isotopic Ratios of IHSS Samples. International Humic Substances Society Website. Retrieved 6/26/2013 from <<http://www.humicsubstances.org/sources%20-%20PonyLake.html>>.
- Johnson, I. D., 2010. The molecular probes handbook: a guide to fluorescent probes and labeling technologies, 11th Edition. Life Technologies Corporation.
- Katsoyiannis I.A., Canonica S., von Gunten U., 2011. Efficiency and energy requirements for the transformation of organic micropollutants by ozone, O<sub>3</sub>/H<sub>2</sub>O<sub>2</sub> and UV/H<sub>2</sub>O<sub>2</sub>. *Water Research* 45 (13), 3811-3822.
- McKay G., Dong M.M., Kleinman J.L., Mezyk M.P., Rosario-Ortiz F.L., 2011. Temperature dependence of the reaction between the hydroxyl radical and organic matter. *Environmental Science & Technology* 45 (16), 6932-6937.
- McKay, G., Kleinman, J.L., Johnston, K.M., Dong, M.M., Rosario-Ortiz, F.L., Mezyk, S.P., 2013. Kinetics of the reaction between the hydroxyl radical and organic matter standards from the International Humic Substance Society. *Journal of Soils and Sediments*, 1-7.

- Mostofa, K.M., Liu, C.Q., Sakugawa, H., Vione, D., Minakata, D., Saquib, M., Mottaleb, M.A., 2013. Photoinduced generation of hydroxyl radical in natural waters. *Photobiogeochemistry of Organic Matter* 209-272.
- Ou, B., Hampsh-Woodill, M., Flanagan, J., Deemer, E. K., Prior, R. L., Haung, D., 2002. Novel fluorometric assay for hydroxyl radical prevention capacity using fluorescein as the probe. *Journal of Agricultural Food Chemistry* 50 (10), 2772-2777.
- Prahl, S., 2013. Optical absorption of methylene blue. Oregon Medical Laser Center Website. Retrieved 7/12/2012 from < <http://omlc.ogi.edu/spectra/mb/index.html>>.
- Rosario-Ortiz, F.L., Mezyk, S.P., Doud, D.F., Snyder, S.A., 2008. Quantitative correlation of absolute hydroxyl radical rate constants with non-isolated effluent organic matter bulk properties in water. *Environmental Science & Technology* 42 (16), 5924-5930.
- Rosenfeldt, E.J., Linden, K.G., 2004. Degradation of endocrine disrupting chemicals bisphenol a, ethinyl estradiol, and estradiol during UV photolysis and advanced oxidation processes. *Environmental Science and Technology* 38, 5476-5483.
- Sharp E.L., Parsons, S.A., Jefferson, A., 2006. Seasonal variations in natural organic matter and its impact on coagulation in water treatment. *Science of the Total Environment* 363, 183-194.
- Sigma Aldrich Co. Llc. 2013.<sup>a</sup> Fluorescein sodium salt. Sigma Aldrich Website. Retrieved August 6, 2013 from < <http://www.sigmaaldrich.com/catalog/product/sial/f6377?lang=en&region=US>>.
- Sigma Aldrich Co. Llc. 2013.<sup>b</sup> Methylene blue. Sigma Aldrich Website. Retrieved August 6, 2013 from < <http://www.sigmaaldrich.com/catalog/product/sial/m9140?lang=en&region=US>>.
- Thorn, K.A., Folan, D.W., MacCarthy, P., 1989. characterization of the international humic substances society standard and reference fulvic and humic acids by solution state carbon-13 (<sup>13</sup>C) and hydrogen-1 (<sup>1</sup>H) nuclear magnetic resonance spectrometry. U.S. Geological Survey, Water-Resources Investigations Report 89-4196, Denver, CO, 93 pp.
- The United States Pharmacopeial Convention, 2008. Methylene Blue (Veterinary—Systemic). Texas A&M Veterinary Medicine and Biomedical Sciences Website. Retrieved 7/12/2012 from <<http://vetmed.tamu.edu/common/docs/public/aavpt/methyleneBlue.pdf>>.
- vonGunten, U., 2003. Ozonation of drinking water: part I: oxidation kinetics and product formation. *Water Research* 37 (7), 1443e1467.

## Chapter 4: Conclusions

- The R-SAM method has demonstrated capabilities to perform rapid (<1 hour) scavenging measurements in a portable field-deployable setup.
- Long term measurement of •OH scavenging in water treatment plants demonstrated short term ( $\approx$  one month) stability of first and second order NOM scavenging rates but significant seasonal variability of NOM loading rates and erratic variability of NOM-•OH reaction rate constants. NOM loading, however was the dominant contributor to scavenging variability.
- Surface water showed evidence of a relationship between heavy rainfall, elevated scavenging rates, and increased apparent NOM-•OH reaction rate constants.
- Adjusting scavenging design levels in AOP systems in response to periodically measured scavenging levels was predicted to reduce energy consumption by 41% with higher certainty of treatment in subject Plant 2, as compared to a constant scavenging assumption.
- A six-point criteria scheme was developed to guide •OH probe selection for R-SAM measurements.
- The R-SAM accurately reproduced published measurements of the •OH scavenging rate constant for the NOM isolate ESHA-S but results were strikingly different than previous work for PLFA-R and SRHA II-S. The range of R-SAM results for NOM isolates, however, is in general agreement with most available literature.



- Consistent with previous work, no statistically significant relationships were evident when correlating scavenging rates with weight averaged molecular weight, bulk elemental composition, or ratio of aliphatic to aromatic carbon.
- Observations about the potential impacts of non-ideal behavior of reactions between reagents and transport limitations of  $\bullet\text{OH}$  reactions indicate additional research should be performed to fully validate competition kinetics scavenging analysis schemes involving fast reacting reagents.

Based on this research, it is clear that there is significant as yet unpredictable variability of NOM scavenging behavior over time in the environment as well as between standard NOM isolates. It is evident that understanding the relationship between NOM variables and scavenging behavior will require advanced analytical techniques including, multivariate analyses, NOM fractioning, or perhaps advanced mathematical models of continuous NOM variables as proposed here. In the interim, however, the R-SAM method has demonstrated its adaptability to multiple applications and could be further developed to meet the needs of  $\bullet\text{OH}$  scavenging prediction in a wide array of contexts.

## Appendix: Detailed R-SAM procedure.

### Required Equipment:

- R-SAM equipment
- Computer running Microsoft *Windows* Operating System
- Microsoft *Excel* Software
- R-SAM *Excel* spreadsheet (included with R-SAM equipment)
- GraphPad *Prism* Software
- Avantes *AvaSoft* software (included with R-SAM equipment)
- 500ml glass graduated cylinder
- 250ml glass Erlenmeyer flask
- 100ml glass beaker (included with R-SAM equipment)
- 0-10,000  $\mu\text{L}$ , 0-250  $\mu\text{L}$  pipette
- Pipetteboy with 50 ml tip.
- 10mm stir bars (x10) (included with R-SAM equipment)

### Stock Solutions:

- 1 mM Probe Dye (Sodium Fluorescein or Methylene Blue)
- 10% tertiary butyl alcohol (t-BuOH)
- 99.9+% Hydrogen Peroxide ( $\text{H}_2\text{O}_2$ )
- Sample water (>.6L)
- 1M NaOH

### Step 1: Warm up lamps

- Turn on HAL lamp and R-SAM UV fixture –ensure R-SAM bulbs are not flickering by turning lamps on and off a few times.
- Allow both lamps to warm while performing steps 2-4

### Step 2: Set up data export

- Open the AvaSoft application.
- In the Application menu select Excel Output, and then Settings.
- Under the Select Mode option box, select Export a fixed number of scans to Excel.
- Under Export Mode enter the 254 for the desired number of scans and 0 for the time interval between scans. The interval may need to be adjusted to accommodate higher scavenging samples and higher concentrations of t-BuOH.
- In Application menu, select Enable under Excel Output.
- In the Application menu select History, then Function Entry.

- On the F1 tab, under Function Type select View Spectrum and under Measure Mode select Absorbance.
- Under Function Definition enter 663.8-664.5nm for Methylene blue and 459.5-460.5nm for Sodium Fluorescein in the wavelength range fields. Leave Master for the Spectrometer Channel.
- Choose to Display no peaks.

### Step 3: Prepare 0 $\mu\text{M}$ t-BuOH test solution

- Fill graduated cylinder with  $\approx$ 100ml sample water.
- Add
  - 500  $\mu\text{L}$  of 1 mM methylene blue probe dye stock.
  - 2,500  $\mu\text{L}$  of 1 mM sodium fluorescein probe dye stock.
- Add 30.2 mL of  $\text{H}_2\text{O}_2$  stock.
- Fill cylinder to 500ml mark to make final concentration of 1 $\mu\text{M}$ /5 $\mu\text{M}$  methylene blue/sodium fluorescein and 20mg/L  $\text{H}_2\text{O}_2$ .
- If using sodium fluorescein, adjust pH to  $>8.4$  using NaOH while stirring (should require less than 50 $\mu\text{L}$  of NaOH).
- Stir solution—can use 50 ml pipetteboy tip to stir.

### Step 4: Make 1,000 $\mu\text{M}$ t-BuOH solution

- Add 95.6  $\mu\text{L}$  of t-BuOH stock solution to the 250 ml Erlenmeyer flask.
- Rinse the pipetteboy tip with  $\approx$ 55 ml of the 0  $\mu\text{M}$  test solution from Step 3 three times, returning solution to graduated cylinder after each rinse. Then, using the pipetteboy, transfer 100 mL of the 0 $\mu\text{L}$  solution to the 250ml Erlenmeyer flask.
- Stir solution –can use tip from 0-10,000  $\mu\text{L}$  pipette.

### Step 5: Zero Spectrophotometer

- Add 40 mL of sample water to 100ml beaker and place in metal R-SAM reactor collar.
- Align the right edge of the white label field on the beaker with the set screw that runs perpendicular to the path of light from the HAL to the spectrophotometer lens –the other screws have lock nuts on them to ensure only the one screw can be adjusted, facilitating consistent reactor placement. Orientation of the beaker may have to be modified to ensure the light path is not blocked when using other equipment, however, it is important to ensure consistent beaker orientation between apparent rate constant measurements.
- Open the *AvaSoft* application with the spectrophotometer USB cable plugged in.

- In the *AvaSoft* window click the 'Start' button to display the current spectrophotometer readings at all wavelengths.
- The integration time must be adjusted in the box on the task bar to ensure the maximum count at 664/460nm, for Methylene Blue and Sodium Fluorescein respectively, is roughly 90% of the full count (vertical) axis –about 56,000 counts. Stopping and starting the spectrophotometer allows the new integration time to take effect. With the integration time set, there will still be some oversaturated wavelengths. This is not a problem.
- With the halogen light, and UV bulbs having been on continuously for > 3 minutes, click the white square in the task bar to record the 100% transmittance reference.
- Turn off the halogen light source, leave the UV lamp on, and click the black square to record the 0% transmittance.
- Any future adjustments to integration time, or the position of the reactor beaker, fiber optic cables or integration time may require recording new transmittance references. The current integrity of the reference data can be determined by confirming that the oversaturated wavelengths when viewed in the scope (S) view read zero in the absorbance (A) view.
- Switch to the absorbance mode by clicking the A button.
- Pour sample water back into sample bottle to use for potential re-zeroing later on.

#### **Step 6: Perform Measurements**

- Apparent degradation rates for the probe dye must be measured in sample water with each of several concentrations of t-BuOH. These concentrations are achieved by mixing appropriate volumes of the solutions from Steps 3 and 4 in the 100ml beaker (Table 4). Use the 50 ml pipette for the 0  $\mu$ M t-BuOH solution from Step 3, and the 0-10,000  $\mu$ L pipette for the 1,000  $\mu$ L t-BuOH solution from Step 4. The best results have been achieved by starting at the middle t-BuOH concentrations, and moving towards the high and low concentrations on alternate measurements.

[T-BuOH]	Vol. 1,000 $\mu\text{M}$ t-BuOH Solution (ml)	Vol. 0 $\mu\text{M}$ t-BuOH Solution (ml)
0 $\mu\text{M}$	0	0
10 $\mu\text{M}$	.4	39.6
25 $\mu\text{M}$	1	1
50 $\mu\text{M}$	2	2
100 $\mu\text{M}$	4	4
150 $\mu\text{M}$	6	6
250 $\mu\text{M}$	10	10
400 $\mu\text{M}$	16	16
500 $\mu\text{M}$	20	20
750 $\mu\text{M}$	30	10
1,000 $\mu\text{M}$	40	0

**Table 4: R-SAM measurement t-BuOH mixing volumes.**

- Once 0 and 1,000  $\mu\text{M}$  t-BuOH solutions have been mixed to achieve the desired concentration, add a stir bar using clean tweezers, pull the reactor collar from under the UV light source, set the beaker in place and tighten the set screw perpendicular to the spectrophotometer light path.
- Cover the beaker with the shutter plate and push into position under the UV light source.
- With AvaSoft running in absorbance mode, observe that the oversaturated areas of the spectrum are reading zero. Small adjustments to the set screw, and fiber optic cables can be made to move these flat sections of the absorbance curve up and down.
- If the flat sections will not zero with reasonable adjustments of the set screw or fiber optic cables, pour out the solution and re-zero the instrument using as in Step 5.
- With acceptable zeroing confirmed, simultaneously pull the shutter plate off the beaker and press Start Measuring under History in the Application menu in AvaSoft. AvaSoft will open a workbook in Excel and begin recording absorbance data.
- Each measurement run will take approximately 0.5-5 minutes depending on integration time and data export rate. Actual time period can be determined by watching the Excel file generated by AvaSoft populate. When column IU populates, measurement is complete. Note: Do not click any Excel menu, button or cell during measurement as this will disrupt data recording.
- Once the measurement is complete, save the file with a name that indicates the sample ID, date, and specific t-BuOH concentration.
- Discard the used test solution and rinse the beaker three times with deionized water before measuring degradation rate in the next concentration of t-BuOH. It is important to ensure cleanliness of the beaker and stir bars between measurements by thorough

rinsing to prevent cross contamination. Drying is not required, although it is recommended to tap out as much rinse water as possible prior to mixing up a new t-BuOH concentration.

- Running 12 t-BuOH concentrations has demonstrated good results, however, there is room to optimize the range of concentrations used, and number of replicates that are needed.

### Step 7: Review Data

- As apparent rate constant measurements are made at different concentrations of t-BuOH, data from each Excel file can be copied into the R-SAM spreadsheet, data fields, while filling in the specific concentration of t-BuOH for each measurement.
- When reviewing data, ensure more than 20% degradation is being captured by confirming that the value of  $-\ln([\text{probe}]_t/[\text{probe}]_0)$  in column IU is greater than .223. More degradation can be captured by increasing the time interval between scans in the Settings dialogue box under Excel Output in the Application menu. Shorter integration time, however, increases precision, so it is advisable not to increase integration time unless it's necessary. The extent of degradation captured for a given time interval setting varies with t-BuOH concentration and background scavenging level, so the time interval time may have to be adjusted periodically throughout an analysis. AvaSoft only accepts integer inputs in the time interval column, where zero indicates the fastest possible data export rate.
- It is important to review data prior to discarding 0 and 1,000  $\mu\text{M}$  t-BuOH solutions to detect aberrant values and perform replicates of those data. The R-SAM workbook provides a graphical display of the preliminary results using a linearized analysis. Viewing the Chart tab allows ongoing review of data as individual rate measurement data is copied into the file. By adjusting the data displayed you can evaluate the linearity of the apparent rate constant measurements. If sufficient 0 and 1,000  $\mu\text{M}$  t-BuOH solutions remain, it is beneficial to re-run outlying concentrations. NOTE: it is important to include all data unless there is an identifiable cause for error. Also, on occasion, the premixed solutions become contaminated and all subsequent measured apparent probe degradation rate constants deviate from linearity. In such cases, it is appropriate to exclude all data taken from the first departure from linearity onward.

### Step 8: Analyze Data

- With all data collected, prepare a table with [t-BuOH],  $k_{app}$ , and standard error of  $k_{app}$  as columns 1-3 respectively.
- In *Prism*, open a New XY table from the sidebar on the startup page.
- Under the enter Y data section chose Enter and Plot error values already calculated elsewhere and select Mean with SEM from the dropdown.
- In the analysis group in the task bar, chose Fit a curve with non linear regression. Click the plus to the right of the main dialogue box to fit a new equation, name the equation and enter an equation of the form of Equation 8.

$$k_{MB}^{app} = \frac{k_{\bullet OH, MB} \times \alpha_{\bullet OH}}{\sum_i [Scav_i] k_{\bullet OH, Scav_i} + k_{\bullet OH, t-BuOH} [t-BuOH] + k_{\bullet OH, MB} [MB] + k_{\bullet OH, H_2O_2} [H_2O_2]} \quad (8)$$

Where

$k_{\bullet OH, probe} = 1.2 \times 10^{10} \text{ M}^{-1} \text{ s}^{-1}$  for methylene blue,  $1.16 \times 10^{10} \text{ M}^{-1} \text{ s}^{-1}$  for sodium fluorescein;

$$k_{\bullet OH, t-BuOH} = 6 \times 10^8 \text{ M}^{-1} \text{ s}^{-1}$$

$$k_{\bullet OH, H_2O_2} = 2.7 \times 10^7 \text{ M}^{-1} \text{ s}^{-1}$$

[probe] =  $1 \times 10^{-6} \text{ M}$  for methylene blue,  $5 \times 10^{-6} \text{ M}$  for sodium fluorescein

$$[H_2O_2] = 5.88 \times 10^{-4} \text{ M} (=20 \text{ mg/L})$$

- After entering Equation 8, select the Rules for Initial Values tab, set A to  $9 \times 10^{-8}$  and E to 60,000 and press Okay.
- At the main Parameters for Nonlinear Regression screen select automatic outlier elimination in the Fitting Method screen.
- Under the weights tab, enter 5% in the Q= box and select No weighting in the Weighting method section and press Okay at the bottom right.
- *Prism* will generate a new table under Results in the left sidebar. This table contains the most likely value for scavenging,  $\bullet OH$  production rate, and detailed error and quality of fit statistics.

## Comprehensive Bibliography

- Asmus, K.D., 1984. Pulse Radiolysis Methodology. *Methods of Enzymology* 105, 167-178.
- Banat, F., Al-Asheh, S., Al-Rawashdeh, M., Nusair, M., 2005. Photodegradation of methylene blue dye by the UV/H<sub>2</sub>O<sub>2</sub> and UV/acetone oxidation processes. *Desalination* 181 (1), 225-232.
- Buxton, G.V., Greenstock, C.L., Helman, W.P., Ross, A.B., 1988. Critical review of rate constants for reactions of hydrated electrons, hydrogen atom and hydroxyl radicals ( $\bullet\text{OH}/\bullet\text{O}$ ) in aqueous solutions. *Journal of Physical Chemistry Reference Data* 17, 513–886.
- Buxton, G.V., Stuart, C.R., 1995. Re-evaluation of the thiocyanate dosimeter for pulse radiolysis. *Journal of the Chemical Society, Faraday Transactions* 91 (2), 279-281.
- Bolton, J.R., Linden, K.G., 2003. Standardization of Methods for Fluence (UV Dose) Determination in Bench-Scale UV Experiments. *Journal of Environmental Engineering* 129 (3), 209-215.
- Comninellis, C., Kapalka, A., Malato, S., Parsons, S., Poullos, I., Mantzavinos, D., 2008. Advanced Oxidation Processes for Water Treatment: Advances and Trends for R&D. *Journal of Chemical Technology and Biotechnology* 83 (6), 769–776.
- Cordier, P., Grossweiner, L.I., 1968) Pulse radiolysis of aqueous fluorescein. *Journal of Physical Chemistry*. 72(6) 2018-2026.
- Dong, M.M., Mezyk, S.P., Rosario-Ortiz, F.L., 2010. Reactivity of effluent organic matter (EfOM) with hydroxyl radical as a function of molecular weight. *Environmental Science and Technology*, 44, 5714–5720.
- Dorfman, L.M., Adams, G.E., 1973. Reactivity of the Hydroxyl Radical, National Bureau of Standards, Report No. NSRDS-NBS-46.
- EPA, 1998. Handbook on Advanced Photochemical Oxidation Processes. US Environmental Protection Agency, EPA/625/R-98/004, Cincinnati, Ohio 45266.
- Espulgas, S., Bila, D.M., Krause, L.G.T., Dexotti, M., 2007. Ozonation and Advanced Oxidation Technologies to Remove Endocrine Disrupting Chemicals (EDCs) and Pharmaceuticals and Personal Care Products (PPCPs) in Water Effluents. *Journal of Hazardous Materials* 149 631-642.
- Flyunt, R., Leitzke, A., Mark, G., Mvula, E., Reisz, E., Schick, R., von Sonntag, C., 2003. Determination of  $\bullet\text{OH}$ ,  $\text{O}_2\bullet^-$ , and hydroperoxide yields in ozone reactions in aqueous solution. *Journal of Physical Chemistry B* 107 (30), 7242-7253.
- Goldstone, J.V., Pullin, M.J., Bertilsson, S., Voelker, B.M., 2002. Reactions of hydroxyl radical with humic substances: bleaching, mineralization, and production of bioavailable carbon substrates. *Environmental Science and Technology* 36 (3), 364-372.



- Hao, X.L., Zhou, M.H., Zhang, Y., Lei, L.C., 2006. Enhanced degradation of organic pollutant 4-chlorophenol in water by non-thermal plasma process with TiO<sub>2</sub>. *Plasma Chemistry and Plasma Process* 26 (5), 455–468.
- Hoigné, J., Bader, H., Haag, W.R., Staehelin, J., 1985. Rate constants of reactions of ozone with organic and inorganic compounds in water—III. Inorganic compounds and radicals. *Water Research*, 19 (8), 993-1004.
- Hross, M.H., 2010. Rapid measurement of background hydroxyl radical scavenging in water: Masters Project. University of Massachusetts – Amherst, Department of Civil and Environmental Engineering.
- Hynes, A. J., Wine, P.H., Semmes, D.H., 1986. Kinetics and mechanism of hydroxyl reactions with organic sulfides. *Journal of Physical Chemistry* 90 (17), 4148-4156.
- IHHS 2013.<sup>a</sup> Pony Lake Fulvic Acid: A microbially-derived fulvic acid collected from a hypereutrophic coastal pond in Antarctica. International Humic Substances Society Website. Retrieved 6/26/2013 from <<http://www.humicsubstances.org/elements.html>>.
- IHHS 2013.<sup>b</sup> Elemental Compositions and Stable Isotopic Ratios of IHSS Samples. International Humic Substances Society Website. Retrieved 6/26/2013 from <<http://www.humicsubstances.org/sources%20-%20PonyLake.html>>.
- Jayson, G.G., Parsons, B.J., 1973. Some simple, highly reactive, inorganic chlorine derivatives in aqueous solution. *Journal of the Chemical Society, Faraday Transactions 1: Physical Chemistry in Condensed Phases* 69, 1597–1607.
- Johnson, I. D., 2010. *The molecular probes handbook: a guide to fluorescent probes and labeling technologies*, 11th Edition. Life Technologies Corporation.
- Katsoyiannis I.A., Canonica S., von Gunten U., 2011. Efficiency and energy requirements for the transformation of organic micropollutants by ozone, O<sub>3</sub>/H<sub>2</sub>O<sub>2</sub> and UV/H<sub>2</sub>O<sub>2</sub>. *Water Research* 45 (13), 3811-3822.
- Kolpin, D.W., Furlong E.T., Neyer, M.T., Thurman, M., Zaugg, S.D., Barber, L.B. Buston, H.T., 2002. Pharmaceuticals, hormones, and other organic wastewater contaminants in U.S. streams, 1999–2000: A national reconnaissance. *Environmental Science and Technology* 36 (6), 1202-1211.
- Lee, Y., von Gunten, U., 2010. Oxidative transformation of micropollutants during municipal wastewater treatment: comparison of kinetic aspects of selective (chlorine, chlorine dioxide, ferrate VI and ozone) and non-selective oxidants (hydroxyl radical). *Water Research* 44 (2), 555-556.
- Malins, D.C., Gunselman, S.J., Holmes, E.H., Polissar, N.L., 1993. The etiology of breast cancer characteristic alterations in hydroxyl radical-induced DNA base lesions during oncogenesis with potential for evaluating incidence risk. *Cancer* 71 (10), 3036-3043.

- McKay G., Dong M.M., Kleinman J.L., Mezyk M.P., Rosario-Ortiz F.L., 2011. Temperature dependence of the reaction between the hydroxyl radical and organic matter. *Environmental Science & Technology* 45 (16), 6932-6937.
- McKay, G., Kleinman, J.L., Johnston, K.M., Dong, M.M., Rosario-Ortiz, F.L., Mezyk, S.P., 2013. Kinetics of the reaction between the hydroxyl radical and organic matter standards from the International Humic Substance Society. *Journal of Soils and Sediments*, 1-7.
- Moncayo-Lasso, A., Mora-Arismendi, L.E., Rengifo-Herrera, J.A., Sanabria, J., Benitez, N., Pulgarin, C., 2012. The detrimental influence of bacteria (*E. coli*, *Shigella* and *Salmonella*) on the degradation of organic compounds (and vice versa) in TiO<sub>2</sub> photocatalysis and near-neutral photo-Fenton processes under simulated solar light. *Photochemical and Photobiological Sciences* 11 (5), 821-827.
- Mostofa, K.M., Liu, C.Q., Sakugawa, H., Vione, D., Minakata, D., Saquib, M., Mottaleb, M.A., 2013. Photoinduced generation of hydroxyl radical in natural waters. *Photobiogeochemistry of Organic Matter* 209-272.
- Motulsky, H.J., Brown R.E., 2006. Detecting outliers when fitting data with nonlinear regression—a new method based on robust nonlinear regression and the false discovery rate. *BMC bioinformatics* 7 (1) 123.
- Notre Dame Radiation Laboratory, 2002. Radiation Chemistry Data Center, Kinetics Database. [www.rccd.nd.edu](http://www.rccd.nd.edu) (accessed March 10, 2008).
- Ou, B., Hampsh-Woodill, M., Flanagan, J., Deemer, E. K., Prior, R. L., Haung, D., 2002. Novel fluorometric assay for hydroxyl radical prevention capacity using fluorescein as the probe. *Journal of Agricultural Food Chemistry* 50 (10), 2772-2777.
- Peternel, I.T., Koprivanac N., Bozic, A.M.L., Kusic, H. M., 2007. Comparative study of UV/TiO<sub>2</sub>, UV/ZnO and photo-Fenton processes for the organic reactive dye degradation in aqueous solution. *Journal of Hazardous Materials* 148 (1), 477–484.
- Poeggeler, B., Reiter, R.J., Tan, D.X., Chen, L.D., Manchester, L.C., 1993. Melatonin, hydroxyl radical-mediated oxidative damage, and aging: A hypothesis. *Journal of Pineal Research* 14 (4), 151-168.
- Prahl, S., 2013. Optical absorption of methylene blue. Oregon Medical Laser Center Website. Retrieved 7/12/2012 from < <http://omlc.ogi.edu/spectra/mb/index.html>>.
- Rosario-Ortiz, F.L., Mezyk, S.P., Doud, D.F., Snyder, S.A., 2008. Quantitative correlation of absolute hydroxyl radical rate constants with non-isolated effluent organic matter bulk properties in water. *Environmental Science & Technology* 42 (16), 5924-5930.
- Rosenfeldt, E.J., Linden, K.G., 2004. Degradation of endocrine disrupting chemicals bisphenol a, ethinyl estradiol, and estradiol during UV photolysis and advanced oxidation processes. *Environmental Science and Technology* 38, 5476-5483.

- Rosenfeldt, E.J., Linden, K.G., 2007. The  $R_{OH,UV}$  concept to characterize and the model UV/H<sub>2</sub>O<sub>2</sub> process in natural waters. *Environmental Science and Technology* 41, 2548-2553.
- Sharp E.L., Parsons, S.A., Jefferson, A., 2006. Seasonal variations in natural organic matter and its impact on coagulation in water treatment. *Science of the Total Environment* 363, 183–194.
- Sigma Aldrich Co. Llc. 2013.<sup>a</sup> Fluorescein sodium salt. Sigma Aldrich Website. Retrieved August 6, 2013 from <<http://www.sigmaaldrich.com/catalog/product/sial/f6377?lang=en&region=US>>.
- Sigma Aldrich Co. Llc. 2013.<sup>b</sup> Methylene blue. Sigma Aldrich Website. Retrieved August 6, 2013 from <<http://www.sigmaaldrich.com/catalog/product/sial/m9140?lang=en&region=US>>.
- Sinkkonen, S., Paasivirta, J., 2000. Degradation half-life times of PCDDs, PCDFs and PCBs for environmental fate modeling. *Chemosphere* 40 (9), 943-949.
- Staelin, J., Hoigne, J., 1982. Decomposition of ozone in water: rate of initiation by hydroxide ions and hydrogen peroxide. *Environmental Science and Technology* 16 (10), 676-681.
- Stumm, W., Morgan, J.J., 1996. *Aquatic Chemistry: Chemical equilibria and rates in natural waters*, third ed. Wiley INT Publication, New York.
- Thorn, K.A., Folan, D.W., MacCarthy, P., 1989. characterization of the international humic substances society standard and reference fulvic and humic acids by solution state carbon-13 (<sup>13</sup>C) and hydrogen-1 (<sup>1</sup>H) nuclear magnetic resonance spectrometry. U.S. Geological Survey, Water-Resources Investigations Report 89-4196, Denver, CO, 93 pp.
- Trojan Technologies Inc. 2005. Trojan's UV -oxidation solutions for seasonal taste and odor. Engineering America Website. Retrieved 7/17/2013 from <[http://www.engamerica.com/uploaded/Doc/Trojan\\_Taste\\_and\\_Odor\\_Application\\_Sheet.pdf](http://www.engamerica.com/uploaded/Doc/Trojan_Taste_and_Odor_Application_Sheet.pdf)>
- Tucson Water, 2012. Advanced oxidation process (AOP) water treatment facility fact sheet. City of Tucson Arizona Website. Retrieved 7/5/2013 from <[http://cms3.tucsonaz.gov/sites/default/files/water/docs/071812\\_aop\\_facts.pdf](http://cms3.tucsonaz.gov/sites/default/files/water/docs/071812_aop_facts.pdf)>
- The United States Pharmacopeial Convention, 2008. Methylene Blue (Veterinary—Systemic). Texas A&M Veterinary Medicine and Biomedical Sciences Website. Retrieved 7/12/2012 from <<http://vetmed.tamu.edu/common/docs/public/aavpt/methyleneBlue.pdf>>.
- vonGunten, U., 2003. Ozonation of drinking water: part I: oxidation kinetics and product formation. *Water Research* 37 (7), 1443e1467.

- Weather Underground, Inc., 2013. Weather History for Fredericksburg, VA: Weeks of July 8, 2012 to August 19, 2012. wunderground.com. Retrieved 6/13/2013 from <<http://www.wunderground.com/history/airport/KEZF/2012/8/22/WeeklyHistory.html?MR=1>>.
- Westerhoff, P., Aiken, G., Amy, G., Debroux, J., 1999. Relationships between the structure of natural organic matter and its reactivity towards molecular ozone and hydroxyl radicals. *Water Research* 33 (10), 2265–2276.
- Westerhoff, P., Yoon, Y., Snyder, S., Wert, E., 2005. Fate of endocrine-disruptor, pharmaceutical, and personal care product chemicals during simulated drinking water treatment processes. *Environmental Science and Technology* 39 (17), 6649-6663.
- Westerhoff, P., Mezyk, S.P., Cooper, W.J., Minakata, D., 2007. Electron pulse radiolysis determination of hydroxyl radical rate constants with Suwannee River fulvic acid and other dissolved organic matter isolates. *Environmental Science and Technology* 41 (13), 4640–4646.